

The Polar Express: Optimal Matrix Sign Methods and Their Application to the **Muon** Algorithm

Noah Amsel* David Persson† Christopher Musco‡ Robert Gower§

June 1, 2025

Abstract

Computing the polar decomposition and the related matrix sign function, has been a well-studied problem in numerical analysis for decades. More recently, it has emerged as an important subroutine in deep learning, particularly within the **Muon** optimization framework. However, the requirements in this setting differ significantly from those of traditional numerical analysis. In deep learning, methods must be highly efficient and GPU-compatible, but high accuracy is often unnecessary. As a result, classical algorithms like Newton–Schulz (which suffers from slow initial convergence) and methods based on rational functions (which rely on QR decompositions or matrix inverses) are poorly suited to this context. In this work, we introduce **Polar Express**, a GPU-friendly algorithm for computing the polar decomposition. Like classical polynomial methods such as Newton–Schulz, our approach uses only matrix-matrix multiplications, making it GPU-compatible. Motivated by earlier work of Chen & Chow and Nakatsukasa & Freund, **Polar Express** adapts the polynomial update rule at each iteration by solving a minimax optimization problem, and we prove that it enjoys a strong worst-case optimality guarantee. This property ensures both rapid early convergence and fast asymptotic convergence. We also address finite-precision issues, making it stable in `bf16` in practice. We apply **Polar Express** within the **Muon** optimization framework and show consistent improvements in validation loss on large-scale models such as GPT-2, outperforming recent alternatives across a range of learning rates.

Contents

1	Introduction	2
1.1	The Muon Method	3
1.2	Computing the Polar Factor	4
1.3	Contributions	5
2	Related Work	5
3	Approximations by compositions of polynomials	8

*New York University. noah.amsel@nyu.edu

†New York University and Flatiron Institute. dup210@nyu.edu, dpersson@flatironinstitute.org

‡New York University. cmusco@nyu.edu

§Flatiron Institute. rgower@flatironinstitute.org

4	The Polar Express	9
4.1	Greedy is optimal	9
4.2	Finding the optimal polynomial for each iteration	12
4.3	Upper and lower bounds on the singular values	13
4.4	Finite precision considerations	13
4.5	The algorithm	15
5	Numerical experiments	15
5.1	Convergence of Polar Express	15
5.2	Training GPT-2	17
A	Proof of Theorem 4.1	22
B	Proof of Theorem 4.3	25
C	Proof of equivalence between (7) and (8)	26
D	Remez algorithm	26
E	Initialization for Matrices with Large Spectral Gaps	28
F	Fast Polynomial Iteration for Rectangular Matrices	30
G	Code for Constructing Polynomials of Polar Express	32

1 Introduction

Advanced linear algebra is making its way into deep learning. In particular, efficient algorithms for computing *matrix functions* have found applications in training neural networks: approximations to the matrix-inverse are used in the full Adagrad method [14], the matrix square-root and quarter-root appear as subroutines in the Shampoo optimizer [18, 42], and recently, the matrix sign function has found applications within the Muon-optimizer [6, 5, 23].

While the problem of computing these matrix functions has been studied by numerical analysts for decades, applications in deep learning come with different requirements than those in computational science. For example, it is critical to develop methods that take advantage of GPU-friendly operations like matrix-matrix products and avoid less parallel operations. Moreover, for large models, limiting memory overhead is critical. On the other hand, accuracy is typically less critical in machine learning — the long-standing gold standard of 10^{-16} double precision is overkill in deep learning.

With these new considerations in mind, there is an opportunity for research on tailoring matrix function algorithms specifically for deep learning [2]. In this paper, we take a step in this direction, engineering a state-of-the-art, GPU-friendly algorithm for computing the matrix sign function, or more generally, for computing the *polar decomposition* of a rectangular gradient matrix for updating neural network weights. We apply our new **Polar Express** method to computing the descent direction in the recently popular **Muon** method. In Figure 1 we show how using our **Polar Express** method, when coupled with the **Muon** method, consistently achieves a lower validation loss of GPT-2 model for all learning rates, as compared to recent alternative methods [10, 43, 23].

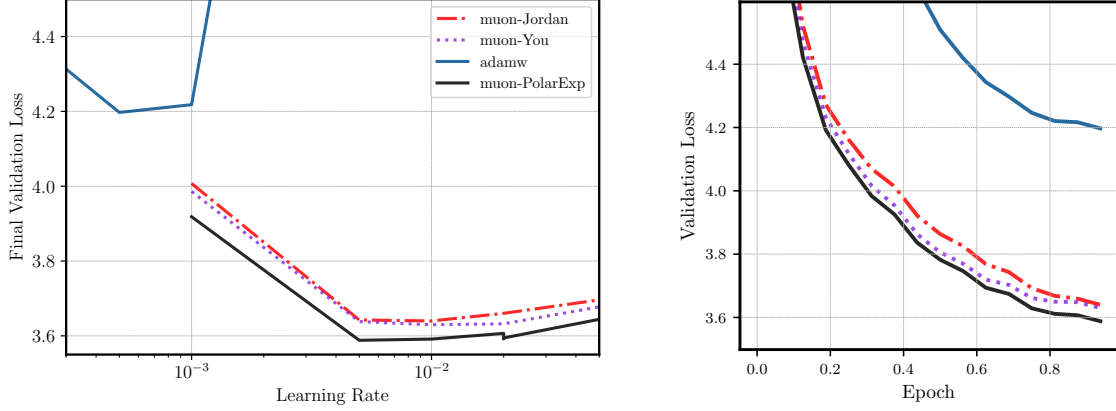


Figure 1: Training a GPT-2 (124M) model on 1 Billion tokens of Fineweb data set [3]. The Legend muon-**<name>** refers to using muon with the **<name>** method for computing the polar. Left: The final Validation loss vs the learning rate and Right: Validation vs iterations for each method with the best resulting learning rate. The final best validation loss for each method, in reverse order was adamw: 4.197, muon-Jordan: 3.639, muon-You: 3.629 and muon-PolarExp: 3.588.

1.1 The Muon Method

Muon has recently gained popularity for training large language models, often outperforming state-of-the-art adaptive gradient methods like Adam and AdamW [27, 32]. Muon has been used to set records for the NanoGPT speedrun [23], and to expand the Pareto frontier for efficient training of large language models [31, 41].

The Muon update rule [6] is defined as follows. Let $\lambda, \beta > 0$ be the learning rate and momentum coefficient hyperparameters. (By default, $\beta = 0.9$.) Let $\mathbf{W}_t \in \mathbb{R}^{m \times n}$ be the weight matrix of a given neural network layer at iteration t , and let $\mathbf{G}_t \in \mathbb{R}^{m \times n}$ be its (stochastic) gradient. Let $\mathbf{M}_t \in \mathbb{R}^{m \times n}$ be the momentum estimate of the gradient, where $\mathbf{M}_0 = \mathbf{0}$. The Muon update is given by

$$\begin{aligned}\mathbf{M}_t &= \beta \mathbf{M}_{t-1} + (1 - \beta) \mathbf{G}_t \\ \mathbf{W}_{t+1} &= \mathbf{W}_t - \lambda \text{polar}(\mathbf{M}_t).\end{aligned}$$

While standard stochastic gradient descent (SGD) with momentum updates the weight matrix by taking a step in the direction $-\mathbf{M}_t$, the Muon method steps in the direction $-\text{polar}(\mathbf{M}_t)$, where $\text{polar}(\mathbf{M})$ denotes the closest semi-orthogonal matrix to \mathbf{M} [20, Chapter 8]. Concretely, if $\mathbf{M} = \mathbf{U}\mathbf{\Sigma}\mathbf{V}^\top$ is the rank-reduced singular value decomposition (SVD) of \mathbf{M} , then

$$\text{polar}(\mathbf{M}) := \mathbf{U}\mathbf{V}^\top. \quad (1)$$

The matrix $\text{polar}(\mathbf{M})$ can be seen as a generalization of the matrix sign function to rectangular matrices [4]. Indeed, when \mathbf{M} is square symmetric with eigendecomposition $\mathbf{M} = \mathbf{V}\mathbf{\Lambda}\mathbf{V}^\top$, $\text{polar}(\mathbf{M})$ exactly coincides with the matrix sign function $\text{sign}(\mathbf{M}) = \mathbf{V} \text{sign}(\mathbf{\Lambda}) \mathbf{V}^\top$ [20, Chapter 10]. Equivalently, $\text{polar}(\mathbf{M})$ is the left orthogonal factor of the polar decomposition of \mathbf{M} [20, Chapter 8]. The motivation for Muon is that the direction $-\text{polar}(\mathbf{M})$ corresponds to the steepest-descent step with respect to the *spectral norm* of the weight matrix \mathbf{W}_t (instead of the Frobenius norm, as in standard SGD). We refer the

reader to [23] or [6] for more information. In this paper, we take the **Muon** update rule for granted and study the problem of computing $\text{polar}(\mathbf{M})$ efficiently.

1.2 Computing the Polar Factor

Although $\text{polar}(\mathbf{M})$ can be computed directly via an SVD in $O(\min(mn^2, nm^2))$ time, doing so is prohibitively expensive in deep learning applications, especially as standard SVD algorithms fail to take full advantage of the parallelism available on GPUs. There has been significant work on highly-parallel methods for the SVD, but the most common approaches compute the matrix-sign function or polar decomposition as a subroutine [34, 36]. Numerical analysts have spent decades developing iterative methods for computing $\text{polar}(\mathbf{M})$. This rich line of work includes Newton–Schulz [20, Chapter 8], Padé iteration [26, 19], the Newton and scaled Newton iterations [20, Chapter 8], the QWHD iteration [33, 36], and Zolo-pd [34]. Unfortunately, as outlined in Section 2, most of these methods are based on rational approximations to the function $\text{sign}(x)$ and require computing matrix inverses or QR decompositions. Such methods are ill-suited to GPU acceleration and deep learning applications. In contrast, the older Newton-Schulz method is based on *polynomial* approximation of $\text{sign}(x)$ and uses only matrix-matrix products. Thus, **Muon** initially used Newton-Schulz [5]. Indeed, **Muon** stands for “MomentUm Orthogonalized by Newton-Schulz” [23].

The Newton-Schulz method constructs a sequence of approximations $\mathbf{X}_t \approx \text{polar}(\mathbf{M})$ as follows:

$$\mathbf{X}_0 = \mathbf{M} / \|\mathbf{M}\|_F \qquad \mathbf{X}_{t+1} = \frac{3}{2}\mathbf{X}_t - \frac{1}{2}\mathbf{X}_t\mathbf{X}_t^\top\mathbf{X}_t \quad (2)$$

At each iteration, this rule effectively applies the cubic polynomial $p(x) = \frac{3}{2}x - \frac{1}{2}x^3$ to the singular values of \mathbf{X}_t . It is well-known that the scalar fixed point iteration $x_{t+1} = p(x_t)$ converges to $\text{sign}(x_0)$ as $t \rightarrow \infty$, provided $|x_0| \leq 1$. As a result, the matrix iteration satisfies $\lim_{t \rightarrow \infty} \mathbf{X}_t = \mathbf{U}\mathbf{V}^\top = \text{polar}(\mathbf{X}_0)$. Higher-degree versions of Newton-Schulz follow the same principle. For example, the degree 5 polynomial $p(x) = (15x - 10x^3 + 3x^5)/8$ can be used to accelerate the convergence. While the Newton-Schulz iteration converges super-exponentially when \mathbf{X}_t is sufficiently close to $\text{polar}(\mathbf{M})$, it suffers from slow initial convergence; when \mathbf{X}_0 is far from $\text{polar}(\mathbf{M})$, the approximation improves slowly over the first few iterations.

In **Muon**, high accuracy approximations to $\text{polar}(\mathbf{M})$ are usually not necessary. The primary goal is instead to compute a coarse approximation in as few iterations as possible. To accelerate convergence in the low-accuracy regime, Jordan recently proposed a fixed-point iteration based on the polynomial $p(x) = 3.4445x - 4.7750x^3 + 2.0315x^5$ [23], which was found using a heuristic numerical search. Unlike Newton-Schulz, the scheme that Jordan proposed does not converge to $\text{polar}(\mathbf{M})$. Instead, it plateaus at an error of ≈ 0.3 . However, it reaches this level of accuracy rapidly. As a result, when the number of iterations is smaller than 10, Jordan’s method outperforms the Newton-Schulz iteration. Building on this idea, You [10] proposed a method that applies six different polynomial updates in succession. This method can achieve somewhat better accuracy than Jordan’s but still fails to converge.

We introduce a new method. In particular, we derive polynomial update rules that are *optimal* at every iteration, outperforming all previous polynomial methods in our setting.

1.3 Contributions

We present **Polar Express**, an iterative method for approximating $\text{polar}(\mathbf{M})$. Our method dynamically adapts the polynomial update rule at each iteration, prioritizing rapid progress in the initial stage and high accuracy in the later stage. **Polar Express** constructs polynomials p_1, \dots, p_T so that the resulting composition is the optimal approximation to the sign function with respect to the supremum (L^∞) norm ([Theorem 4.1](#)). By iteratively applying these polynomials to \mathbf{M} , **Polar Express** inherits a worst-case optimality guarantee for approximating $\text{polar}(\mathbf{M})$ at every iteration. The method converges to $\text{polar}(\mathbf{M})$ super-exponentially ([Theorem 4.3](#)), and it quickly reaches a reasonable approximation in just five or ten iterations. This early-stage acceleration is especially valuable in deep learning applications, where runtime efficiency takes precedence over high accuracy. In contrast, classical methods like Newton-Schulz suffer from a slow initial convergence, while recent heuristic proposals [23, 10] fail to converge. Our method is efficient to run on GPUs, using only a few matrix-matrix products per iteration.

We give an explicit instantiation of **Polar Express** in [Section 4.4](#) with minor modifications to make it compatible with half-precision arithmetic. This formula can be used as a drop-in replacement for previous methods. In numerical experiments, our method outperforms previous methods on synthetic matrices and gradient matrices from a GPT-2 transformer (Fig 4). We demonstrate the effectiveness of **Polar Express** within the Muon algorithm ([Figure 1](#)), showing that it consistently improves the training of GPT-2 language models on 1 billion tokens of the Fineweb dataset [3].

Notation. We let $\|\mathbf{M}\|_F$ and $\|\mathbf{M}\|_2$ denote the Frobenius norm and spectral norm (largest singular value) of a matrix \mathbf{M} , respectively. We denote the spectrum (set of singular values) by $\sigma(\mathbf{M})$.

Let \mathbb{P}_d be the set of polynomials of degree at most d . For odd d , $\mathbb{P}_d^{\text{odd}}$ denotes the set of polynomials of degree at most d containing only odd-degree monomials. For a polynomial p , $\deg(p)$ is its degree. Let $\text{sign}(x)$ be the scalar sign function, which satisfies $\text{sign}(0) = 0$, $\text{sign}(x) = 1$ if $x > 0$ and $\text{sign}(x) = -1$ if $x < 0$.

For a matrix \mathbf{M} with rank reduced SVD given by $\mathbf{M} = \mathbf{U}\mathbf{\Sigma}\mathbf{V}^\top$ and positive singular values $\sigma_1 \geq \dots \geq \sigma_{\text{rank}(\mathbf{M})} > 0$, and a polynomial $p \in \mathbb{P}_d^{\text{odd}}$, we denote by $p(\mathbf{M}) = \mathbf{U}p(\mathbf{\Sigma})\mathbf{V}^\top$, where $p(\mathbf{\Sigma})$ is the diagonal matrix with diagonal entries $p(\sigma_i)$ for $i = 1, \dots, \text{rank}(\mathbf{M})$.

2 Related Work

Computing $\text{polar}(\mathbf{M})$ is an important and longstanding problem in numerical linear algebra, with applications spanning electronic structure calculations, lattice quantum chromodynamics, orthogonal Procrustes analysis, parallel algorithms for computing the SVD, and beyond; see e.g. [19, 24, 9, 17, 37, 44].

The earliest methods in the literature are polynomial iterations like (2). Several nearly simultaneous papers introduced the family of polynomial Padé iterations, comprising Newton-Schulz and its higher-degree analogues [28, 7, 19, 30]. These higher-degree methods are also sometimes called “Newton-Schulz”; when doing so, we will specify the degree for clarity. In these methods, each iteration refines the current approximation \mathbf{X}_t by applying a low-degree odd matrix polynomial, where any odd monomial $x \mapsto x^{2q+1}$ is defined for rectangular matrices by the formula $\mathbf{X}_t \mapsto \mathbf{X}_t (\mathbf{X}_t^\top \mathbf{X}_t)^q$. Our **Polar Express** method

also takes this form, though it changes the polynomial at each iteration. The polynomials used in Padé methods are chosen to match the value and first few derivatives of $\text{sign}(x)$ at the points $x = \pm 1$. For instance, the update rule of the third method in this family is defined by $p(x) = \frac{1}{16}(35x - 35x^3 + 21x^5 - 5x^7)$, which is the unique degree-7 polynomial satisfying $p(\pm 1) = 1$ and $p'(\pm 1) = p''(\pm 1) = p'''(\pm 1) = 0$. These methods converge so long as all singular values of \mathbf{X}_0 lie in $(0, 1]$, a condition guaranteed by the initialization of (2). Furthermore, the order of convergence of the degree $2q + 1$ method is $q + 1$ [7]. In particular, the Newton-Schulz method ($q = 1$) converges quadratically.

In the numerical analysis literature, these polynomial methods were succeeded by rational iterations like Newton's method [19], defined as follows¹:

$$\mathbf{X}_0 = \mathbf{M} \qquad \mathbf{X}_{t+1} = \frac{1}{2} (\mathbf{X}_t + \mathbf{X}_t^{-\top}) \quad (3)$$

Newton's method also converges quadratically, but it uses fewer operations per iteration than Newton-Schulz. Like Newton-Schulz, it works because the rational function $r(x) = \frac{1}{2}(x + x^{-1})$ has a stable fixed point at 1; unlike for Newton-Schulz, this point is a global attractor for the whole positive real line. At first glance, Newton's method has nothing to do with the Padé iterations discussed above. However, after a change of variables $\mathbf{Y}_t = \mathbf{X}_t^{-1}$, it can be reinterpreted as $\mathbf{Y}_{t+1} = 2\mathbf{Y}_t(\mathbf{I} + \mathbf{Y}_t^\top \mathbf{Y}_t)^{-1}$, which is sometimes called inverse Newton. Observing that $r(x) = \frac{2x}{1+x^2}$ satisfies $r(\pm 1) = 1$ and $r'(\pm 1) = 0$, we see that (inverse) Newton is also a Padé method, though a rational rather than polynomial one. In fact, given a odd degree $2q_n + 1$ for the numerator and an even degree $2q_d$ for the denominator, there is a unique rational function that matches the value and first $q_n + q_d$ derivatives of $\text{sign}(x)$ at $x = \pm 1$. This directly yields a Padé method for computing $\text{polar}(\mathbf{M})$ whose order of convergence is $q_n + q_d + 1$. For instance, $r(x) = \frac{x(3+x^2)}{1+3x^2}$ is called Halley's method, which converges cubically. When $q_d = 0$, we recover the polynomial Padé methods.

There are two main weakness of Newton's method and the Padé iterations: slow convergence in the initial phase and the need to compute explicit inverses. To accelerate initial convergence, Higham popularized the technique of rescaling the matrix after every Newton iteration [19]. Intuitively, rescaling \mathbf{X}_t so that $\sigma_{\max} = 1/\sigma_{\min}$ centers the spectrum around 1, where convergence is fastest. Since the (inverse) Newton update treats inputs in the interval $(1/z, 1)$ exactly like those in $(1, z)$, this recentering can only help. Several easily-computable choices of scaling factor exist to accomplish this approximately. Computing matrix inverses is difficult to parallelize and to implement stably in low precision arithmetic. However, a trick was developed for stably computing many rational methods *without* explicit inverses; QR decompositions can be used instead [33, 47]. Applying this trick to Halley's method and combining with a special rescaling scheme yields the QR-based dynamically weighted Halley iteration (QDWH), which converges in just six iterations for any reasonably conditioned matrix [33].

A landmark 2016 paper introduced a new paradigm to design iterative methods for computing $\text{polar}(\mathbf{M})$ [34]. We describe this paradigm in more detail in Section 4, but the main insight is as follows. Padé methods choose the update rule to be an approximation to $\text{sign}(x)$ of a given degree that is optimally accurate in the neighborhood of $x = 1$. Instead, we should choose the approximation to $\text{sign}(x)$ that is optimal over an *interval* $[\ell, 1] \subset \mathbb{R}_{\geq 0}$

¹We describe Newton's method and other rational methods for square non-singular \mathbf{M} . Non-square problems can be reduced to the square case by an initial QR decomposition, but this is not an option for purely polynomial methods like ours.

that contains the singular values. Moreover, after each step of the algorithm, the range of the singular values changes; therefore, we adapt the update rule at each iteration to match the new lower bound ℓ . When the range of the singular values is large, this approach ensures that the update rule shrinks it as quickly as possible. As the algorithm proceeds and the interval shrinks to a small neighborhood of 1, the update rule approaches that of a Padé method, maintaining the same high order of convergence as it has. Within the class of odd rational functions whose numerators and denominators have degree $2q + 1$ and $2q$, respectively, an explicit formula for this optimal approximation to $\text{sign}(x)$ on any interval $[\ell, 1]$ was found by Zolotarev. For $q = 1$, this function coincides exactly with the updates of the dynamically weighted Halley’s method referred to above. It is shown that these rationals have remarkable convergence properties for any q . For even faster convergence than QDWH, the zolo-pd method chooses $q = 17$ [34]. Finally, these methods admit the same QR-based implementation trick as QDWH.

In this paper, we adopt the paradigm of zolo-pd [34] but with polynomials rather than rationals of degree $(2q + 1, 2q)$. This choice avoids the need for QR factorizations, relying solely on GPU-friendly matrix-matrix multiplications in low-precision arithmetic. While this class of methods has not been fully developed in the numerical analysis literature, similar ideas have been rediscovered in different guises. In an unpublished manuscript that predates zolo-pd, Chen and Chow [12] describe a rescaling strategy for Newton-Schulz. Though motivated differently, their method is equivalent to ours for degree-3 polynomials. They also observe numerical instability that prevents the method from converging to all the way to machine precision. Using the insights of [35], they propose a simple mitigation for this issue that we adopt in Section 4.4. Our work gives this method a theoretical foundation that connects it to the paradigm of zolo-pd, and we prove its optimality in the sense of (7). In addition, we study odd polynomials of arbitrary degree and focus particularly on the degree-5 case. Independently, a group of cryptographers developed a similar method for approximating the scalar function $\text{sign}(x)$ in the context of homomorphic encryption schemes [29]. Their focus is mainly on tuning the analogues in their setting of the polynomial degree and number of iterations, whereas we focus on demonstrating optimality and efficiently constructing the update polynomials for degree 3 and 5. In addition, we consider matrix-valued inputs in low-precision arithmetic—not scalars in exact arithmetic—and we demonstrate our method’s effectiveness within the **Muon** algorithm for training deep neural networks.

The designers of **Muon** realized that, due to the extreme efficiency requirements and lax accuracy requirements of their setting, rational-based methods from the numerical analysis literature are inapplicable. However, polynomial-based iteration schemes can take full advantage of GPUs because they use only matrix-matrix products in half-precision arithmetic, not inverses or QR decompositions. The preference for speed over accuracy motivates methods that aim to quickly produce coarse approximations, even at the cost of asymptotic convergence. Examples include the proposals of Jordan [23] and You [43, 10], as discussed in Section 1.2. Like Chen and Chow [12], Jordan found that convergence in the initial phase can be accelerated by choosing update rules that have a large derivative near zero, so as to increase the small singular values as much as possible at each iteration. You furthermore chose to use different update rules at each iteration, allowing extra flexibility to tune the trade-off between speed and accuracy. Both used degree-5 polynomials that were found through gradient descent on heuristic objective functions. These proposals were

compared to Newton-Schultz², but not to Chen and Chow’s method. We find that our method outperforms them all.

3 Approximations by compositions of polynomials

To derive a GPU-friendly method for computing $\text{polar}(\mathbf{M})$, we limit ourselves to the following GPU-friendly operations:

- i) Linear combinations: given scalars $\beta, \gamma \in \mathbb{R}$ and matrices \mathbf{B} and \mathbf{C} , compute $\beta\mathbf{B} + \gamma\mathbf{C}$,
- ii) Matrix-matrix products: compute \mathbf{BC} .

While both these computational primitives are well-suited for parallel computing environments, matrix-matrix products come at a higher computational cost than linear combinations. Therefore, our method attempts to minimize the number of matrix-matrix products. A key observation is that we can compute *odd* monomials of $\mathbf{M} = \mathbf{U}\mathbf{\Sigma}\mathbf{V}^\top$ using the following formula:

$$\mathbf{M}^{2q+1} := \mathbf{U}\mathbf{\Sigma}^{2q+1}\mathbf{V}^\top = \mathbf{M}(\mathbf{M}^\top\mathbf{M})^q.$$

Hence, for an odd polynomial $p(x) = a_0x + a_1x^3 + \cdots + a_qx^{2q+1}$ we can compute

$$p(\mathbf{M}) := a_0\mathbf{M} + a_1\mathbf{M}(\mathbf{M}^\top\mathbf{M}) + \cdots + a_q\mathbf{M}(\mathbf{M}^\top\mathbf{M})^q.$$

Letting ℓ and u be the minimum and maximum singular values of \mathbf{M} , respectively, our goal is now to find an odd polynomial p so that $p(x)$ is as close to 1 as possible on $[\ell, u]$. Indeed, given that $p(\mathbf{M}) - \text{polar}(\mathbf{M}) = \mathbf{U}(p(\mathbf{\Sigma}) - \mathbf{I})\mathbf{V}^\top$, by the unitary invariance of the spectral norm we have that:

$$\|p(\mathbf{M}) - \text{polar}(\mathbf{M})\|_2 \leq \max_{x \in [\ell, u]} |p(x) - 1|. \quad (4)$$

It has been shown that for an arbitrary polynomial p , one requires $\Theta(\deg(p)^{1/2})$ products to compute $p(\mathbf{M})$ [40]; see also [21] for related work. This compares favorably to the naive approach that forms all monomials in p and then sums them together, which requires $\Omega(\deg(p))$ products. However, if p can be expressed as a composition of T polynomials, each of degree d

$$p = p_T \circ p_{T-1} \circ \cdots \circ p_1, \quad (5)$$

then the degree of p is d^T , and $p(\mathbf{M})$ can be efficiently computed recursively by

$$\mathbf{X}_0 = \mathbf{M}, \quad \mathbf{X}_t = p_t(\mathbf{X}_{t-1}) \text{ for } t = 1, 2, \dots, T. \quad (6)$$

The final iterate is $\mathbf{X}_T = p(\mathbf{M})$, which we compute with just $O(Td)$ matrix-matrix products.

Iterative methods for $\text{polar}(\mathbf{M})$ can be seen in this light. For instance, the degree-5 Newton-Schulz method uses the polynomial update $p_t(x) = \frac{15}{8}x - \frac{10}{8}x^3 + \frac{3}{8}x^5$ for each $t = 1, \dots, T$. The composition $p = p_T \circ \cdots \circ p_1$ approximates $\text{sign}(x)$, and the approximation

²Jordan[23] actually compares to $2x - \frac{3}{2}x^3 + \frac{1}{2}x^5$, whereas the true degree-5 Newton-Schulz iteration is $(15x - 10x^3 + 3x^5)/8$. However, the difference in performance is negligible for the first few iterations.

error goes to 0 as T grows. In this paper, we ask the following question: what choice of $p_T \circ \dots \circ p_1$ gives the *best* approximation to $\text{sign}(x)$?

The method we will present is optimal in the following sense: given lower and upper bounds ℓ and u on the singular values of \mathbf{M} , an odd degree $d \in \mathbb{N}$, and the number of iterations $T \in \mathbb{N}$, our method computes the composition $p^*(\mathbf{M})$ that minimizes the worst-case error in the spectral norm. That is,

$$p^* = \underset{\substack{p=p_T \circ p_{T-1} \circ \dots \circ p_1 \\ p_t \in \mathbb{P}_d^{\text{odd}}}}{\text{argmin}} \max_{\substack{\mathbf{M} \in \mathbb{R}^{m \times n} \\ \sigma(\mathbf{M}) \subset [\ell, u]}} \|\text{polar}(\mathbf{M}) - p(\mathbf{M})\|_2. \quad (7)$$

By the unitary invariance of the spectral norm, we have that (7) is equivalent to

$$p^* = \underset{\substack{p=p_T \circ p_{T-1} \circ \dots \circ p_1 \\ p_t \in \mathbb{P}_d^{\text{odd}}}}{\text{argmin}} \max_{x \in [\ell, u]} |1 - p(x)|. \quad (8)$$

For completeness, the equivalence is verified in [Appendix C](#). In other words, the problem given in (7) reduces to that of finding a “uniform” or “minimax” approximation to the constant function $x \mapsto 1$ over the interval $[\ell, u]$, as given in (8). Uniform approximation on an interval by polynomials or rational functions of a given degree is a central topic in approximation theory; see e.g. [45]. Here, we seek an approximation of a particular form—a *composition* of odd polynomials of fixed degrees. In the next section, we solve the optimizing problem of (8) and use the solution to create **Polar Express**.

4 The Polar Express

4.1 Greedy is optimal

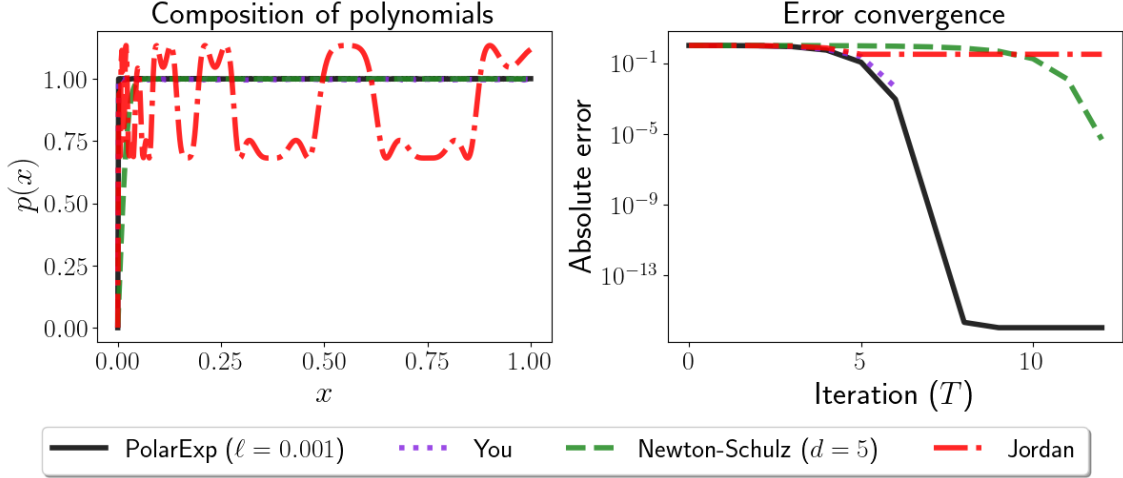
Our key observation is that the polynomial used in each step can be chosen greedily, given the choice of polynomials from the previous iterations. For the first iteration, we choose p_1 so as to map the interval $[\ell, u]$ as close to 1 as possible. That is, it minimizes $\max_{x \in [\ell, u]} |1 - p_1(x)|$. The image of p_1 will be a new interval $[\ell_2, u_2]$, where

$$\ell_2 = \min_{x \in [\ell, u]} p_1(x) \quad u_2 = \max_{x \in [\ell, u]} p_1(x) \quad (9)$$

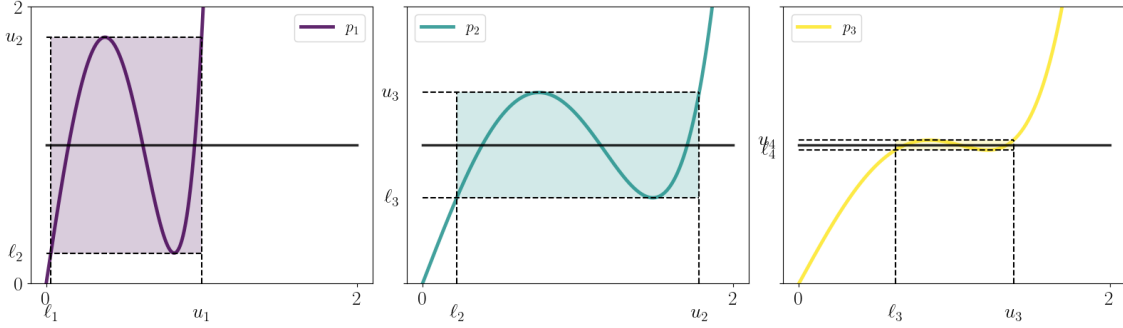
We now pick p_2 to map the interval $[\ell_2, u_2]$ as close to 1 as possible, obtaining a new interval $[\ell_3, u_3]$ that is the image of $[\ell, u]$ through $p_2 \circ p_1$. We continue this process for as many iterations as desired. This same idea was used in zolo-pd [34] to approximate $\text{polar}(\mathbf{M})$ by a composition of rational functions; here we use a composition of polynomials.

The following theorem guarantees that this process finds the solution to (8), and thereby also (7). The scheme is also outlined in [Figure 2](#), which demonstrates the evolution of the lower bounds ℓ_t , the upper bounds u_t , and the polynomials p_t throughout the iterations.





(a) The left figure compares the resulting composition (for $T = 6$ and $d = 5$) of polynomials given by **Polar Express** ($\ell = 0.001$), **You's method** (which is defined up to 6 iterations), **Newton-Schulz**, and **Jordan's method** for approximating $\text{sign}(x)$. The right figure demonstrates error convergence of the methods. Note the slow initial convergence of the Newton-Schulz method.



(b) The evolution of the first three optimal polynomials p_1 , p_2 , and p_3 and the corresponding lower bounds $\ell_{t+1} = p_t(\ell_t)$ and upper bounds $u_{t+1} = 2 - \ell_{t+1}$, as described in [Theorem 4.1](#). The horizontal black line indicates $y = 1$. The polynomial degree is $d = 5$ and the number of iterations is $T = 3$. We set $\ell_1 = 0.03$ and $u_1 = 1$.

Figure 2

Theorem 4.1. Let d be odd and define $\ell_1 = \ell$ and $u_1 = u$. For $t = 1, \dots, T$ define

$$\begin{aligned}
 p_t &= \underset{p \in \mathbb{P}_d^{\text{odd}}}{\text{argmin}} \max_{x \in [\ell_t, u_t]} |1 - p(x)| \\
 \ell_{t+1} &= \min_{x \in [\ell_t, u_t]} p_t(x) \\
 u_{t+1} &= \max_{x \in [\ell_t, u_t]} p_t(x)
 \end{aligned} \tag{10}$$

Then the new error, lower and upper bounds can be computed through

$$\ell_{t+1} = p_t(\ell_t), \quad u_{t+1} = 2 - \ell_{t+1}, \quad \text{and} \quad \max_{x \in [\ell_t, u_t]} |1 - p_t(x)| = 1 - \ell_{t+1}. \tag{11}$$

Furthermore, the composition $p^* := p_T \circ p_{T-1} \circ \dots \circ p_1$ is optimal and the error is given by:

$$\max_{x \in [\ell, u]} |1 - p^*(x)| = \min_{\substack{p = p_T \circ p_{T-1} \circ \dots \circ p_1 \\ p_t \in \mathbb{P}_d^{\text{odd}}}} \max_{x \in [\ell, u]} |1 - p(x)| = 1 - \ell_{T+1}. \quad (12)$$

Proof. See [Appendix A](#). □

Remark 4.2 (Why a fixed degree?). We note that choice of the degree of each p_1, p_2, \dots, p_T need not be the same for [Theorem 4.1](#) to hold. More generally, one may specify a sequence of degrees d_1, \dots, d_T and define each p_t as

$$p_t = \operatorname{argmin}_{p \in \mathbb{P}_{d_t}^{\text{odd}}} \max_{x \in [\ell_t, u_t]} |p(x) - 1|, \quad \text{for } t = 1, \dots, T.$$

Our theory translates entirely to this more general case. However, for simplicity we assume $d = d_t$ for all $t = 1, \dots, T$. Our setting is similar to that of [\[29\]](#), which considers the closely related problem of choosing the depth T and degrees d_1, \dots, d_T such that p approximates sign up to a prescribed error tolerance while minimizing the number of scalar multiplications. Interestingly, from [\[29, Table 2\]](#) the optimal choice of degrees is $d_t = 5$ for *almost* all iterations. This justifies choosing d to be a constant and our use of $d = 5$ in particular.

Fortunately, [\(11\)](#) shows that once p_t has been found, we can compute the new lower and upper bounds ℓ_{t+1} and u_{t+1} and the approximation error simply by evaluating $p_t(\ell_t)$. Hence, for any *fixed* upper and lower bounds on the singular values of \mathbf{M} , we can *precompute* the polynomials p_1, \dots, p_T and the bounds $[\ell_1, u_1], \dots, [\ell_{T+1}, u_{T+1}]$. Then, applying the iterative procedure of [\(6\)](#), the final iterate \mathbf{X}_T will satisfy the following error bound

$$\|\operatorname{polar}(\mathbf{M}) - \mathbf{X}_T\|_2 = \|\operatorname{polar}(\mathbf{M}) - p^*(\mathbf{M})\|_2 \leq 1 - \ell_{T+1}. \quad (13)$$

From optimality guarantee of [Theorem 4.1](#), we know that our method converges at least as fast as the Newton-Schulz iteration of the same degree. Combining this fact with an existing analysis of Newton-Schulz, we immediately get the following convergence guarantee showing that our method enjoys faster than exponential convergence.

Theorem 4.3. Let \mathbf{M} be a matrix normalized so that $\sigma(\mathbf{M}) \subset [\ell, 1]$. Let $\mathbf{X}_T = p^*(\mathbf{M})$, where p^* is the polynomial from [Theorem 4.1](#) with $d = 2q + 1$. Then, we have

$$\|\operatorname{polar}(\mathbf{M}) - \mathbf{X}_T\|_2 \leq |1 - \ell^2|^{(q+1)^T}. \quad (14)$$

Hence, for $d = 3$ the method converges quadratically and for $d = 5$ the method converges cubically.

Proof. See [Appendix B](#). □

In fact, [Theorem 4.3](#) underestimates how fast our method converges. For degree $d = 5$, our method converges about twice as fast as Newton-Schulz (cf. [\[12, Section 3.1\]](#)). Furthermore, the same analysis applies even if p^* is constructed using a lower bound ℓ

that is, where $\ell' \geq \sigma_{\min}(\mathbf{M}) \geq \ell$. Intuitively, when $\ell = u$, the polynomial p^* coincides exactly with the Newton-Schulz method. Mistakenly setting ℓ in the range (σ_{\min}, u) , we obtain a polynomial whose convergence speed is somewhere between that of the optimal polynomial and Newton-Schulz, so the guarantee of [Theorem 4.3](#) can be extended to it as well (cf. [\[12, Theorem 3.3\]](#)).

4.2 Finding the optimal polynomial for each iteration

[Theorem 4.1](#) shows that we can solve (8) by greedily choosing the optimal approximation $p_t \in \mathbb{P}_d^{\text{odd}}$ for each interval $[\ell_t, u_t]$ for $t = 1, \dots, T$. In this section, we show how to find each p_t . Since we are now focused on just one iteration, we drop the subscripts. Given ℓ and u , we wish to solve the following optimization problem:

$$\operatorname{argmin}_{p \in \mathbb{P}_d^{\text{odd}}} \max_{x \in [\ell, u]} |1 - p(x)| \quad (15)$$

That is, we seek a minimax or uniform approximation of the function $x \mapsto 1$ on $[\ell, u]$ from the set of odd polynomials. (Equivalently, we seek a minimax optimal approximation to $\operatorname{sign}(x)$ on $[-u, -\ell] \cup [\ell, u]$.) Problems of this form are well-studied in approximation theory and numerical analysis. The key mathematical insight underlying the solution is the Equioscillation Theorem, which we state formally for our setting in [Lemma A.1](#). This theorem gives a surprising characterization of the optimal approximant: an odd p is optimal for degree $2q + 1$ if and only if there is a set of $q + 2$ equioscillating points. These are points at which p achieves its maximum approximation error $\pm E$, and for which the sign of the error alternates. Even if E is not known in advance, finding a set of $q + 2$ equioscillating points for a given E serves as a certificate that no better approximation error is achievable. The Equioscillation Theorem is the basis of the Remez algorithm [\[38, 39\]](#), a general tool that can be used to find (nearly) optimal polynomial approximations of a given of any degree to *any* function on any interval. With very minor modifications to handle the constraint that p be odd, Remez can be used to directly solve (15). However, the Remez algorithm is opaque, complex, and difficult to implement correctly. Fortunately, we do not need the Remez algorithm in its full generality to solve our problem. We seek only low degree approximants, and the function we wish to approximate is a constant. For $d = 3$, we can actually derive an explicit, closed form solution to (15) using the Equioscillation Theorem. Up to rescaling, the optimal polynomial turns out to be the same one derived in Chen and Chow by different means [\[12\]](#). For degree $d = 5$, we present [Algorithm 2](#), a much simpler way of solving (15) that is mathematically equivalent to Remez in our setting. This algorithm is implemented in its entirety in [Appendix G](#).

We briefly describe the solution for $d = 3$. We seek a polynomial of the form $p(x) = ax + bx^3$. The Equioscillation Theorem stipulates that p must have an equioscillating set of size 3. For p to achieve its maximum error at a point x , x must be a local extremum of $p(x) - 1$ on the interval $[\ell, u]$. Thus, for x to be eligible for membership in the equioscillating set, it must either be a true local extremum of $p(x) - 1$ that lies in $[\ell, u]$, or else one of the endpoints ℓ, u . However, because p is an odd cubic, it has at most one true local extremum on $\mathbb{R}_{\geq 0}$. Thus, to build an equioscillating set of three points, we must include ℓ, u and p 's unique positive local extremum. This local extremum of p occurs at $\sqrt{\frac{-a}{3b}}$. Therefore, we seek a, b such that

$$p(\ell) = 1 - E \quad p\left(\sqrt{\frac{-a}{3b}}\right) = 1 + E \quad p(u) = 1 - E \quad (16)$$

for some unknown E . This is a system of three equations in three variables. The solution $p(x) = ax + bx^3$ is most easily expressed as follows. Let $p_{\text{NS}}(x) = \frac{3}{2}x - \frac{1}{2}x^3$. Then

$$p(x) = \beta p_{\text{NS}}(\alpha x), \text{ where } \alpha = \sqrt{\frac{3}{u^2 + lu + \ell^2}} \text{ and } \beta = \frac{4}{2 + \ell u(\ell + u)\alpha^3}.$$

We now turn to the degree-5 case. The intuition of [Algorithm 2](#) is as follows. For any fixed set of four points $\ell < q < r < u$, we can find an degree-5 odd polynomial p that satisfies

$$p(\ell) = 1 - E \quad p(q) = 1 + E \quad p(r) = 1 - E \quad p(u) = 1 + E$$

for some E by solving a 4×4 linear system. Likewise, for any fixed degree-5 odd p , we can find its four (or fewer) local extrema on $[\ell, u]$ as follows: they occur at ℓ, u and the roots of p' , which is an even degree-4 polynomials whose roots can be found by the *quadratic* formula. [Algorithm 2](#) simply alternates between these two steps until the points q, r converge. Once they have converged, they form an equioscillating set, so p is the optimal polynomial. For more details, please see [Appendix D](#).

4.3 Upper and lower bounds on the singular values

To instantiate our method, we need upper and lower bounds u and ℓ on the singular values of the input matrix \mathbf{M} . A trivial upper bound is given by $\|\mathbf{M}\|_{\text{F}}$. For $\mathbf{M} \in \mathbb{R}^{m \times n}$ with $n \leq m$, this can overestimate $\sigma_{\max}(\mathbf{M})$ by a factor of \sqrt{n} in the worst case. However in practice, the gradient matrices of the weights of dense linear layers in neural networks tend to have small effective rank [\[46\]](#). Consequently, the Frobenius norm tends to be a reasonably good bound on the spectral norm that is loose only by a small constant factor. For stability and consistency, we rescale the input matrix by setting $\mathbf{X}_0 = \mathbf{M}/\|\mathbf{M}\|_{\text{F}}$ and $u = 1$. This rescaling has no effect on the error of our method.

It is difficult to efficiently find a good lower bound on the smallest singular value, so we are forced to guess. Fortunately, the consequences of a bad guess are not severe. As discussed above, the method will eventually converge for any $\ell \in (0, u]$, and even an order of magnitude error only delays convergence by a few iterations. For matrices stored in floating point arithmetic, the singular values are usually larger than machine precision ϵ_{mach} [\[8\]](#), so a good guess is to set $\ell \approx \epsilon_{\text{mach}}$. In our numerical experiments we work in `bf16`, hence we set $\ell = 10^{-3}$ and $u = 1$. Since we use these bounds for all input matrices, we can precompute the optimal polynomials once and apply them to as many inputs as we want.

4.4 Finite precision considerations

When working in finite-precision arithmetic, especially the half-precision `bf16` format used in deep learning, we must take some care to avoid blowups and other problems due to numerical error. To this end, we make three small changes to the method. These adjustments stabilize the algorithm with a negligible effect on accuracy. Observe that these adjustments can be made in the offline stage by modifying the coefficients of our optimal polynomials.

The first issue arises when numerical round-off creates singular values that are slightly larger than u_t . Our optimal polynomials converge only when the singular values of \mathbf{X}_t are actually less than u_t . In some cases we have $p_t(u_t + \epsilon) > u_{t+1} + \epsilon$, so over many iterations, a

singular value that is slightly too large could end up growing to ∞ instead of converging to 1. (This issue is unlikely to arise for degree 3, 7, 11, 15 \dots , for which $p_t(u_t) = \ell_{t+1} < u_{t+1}$). To fix this issue, we simply replace each polynomial $x \mapsto p_t(x)$ by $x \mapsto p_t(x/1.01)$. This safety factor corrects for round-off errors in previous iterations while only slightly changing the behavior of the polynomial on the interval $[\ell_t, u_t]$, though it does cause the singular values to converge to 0.999998 instead of to 1. To correct for this, the safety factor can be omitted in the final iteration.

The second issue was identified in [35] and addressed in the context of polynomial iterations by Chen and Chow [12]. In general, iterative methods for $\text{polar}(\mathbf{M})$ aim to increase each singular value relative to the largest singular value; while $\sigma_{\min}(\mathbf{X}_0) \ll \sigma_{\max}(\mathbf{X}_0)$, after enough iterations, $\sigma_{\min}(\mathbf{X}_t) \approx \sigma_{\max}(\mathbf{X}_t) \approx 1$. However, the convergence of each singular value to σ_{\max} may not be monotonic. Over the domain $\ell_t \ll u_t$, our optimal polynomial p_t oscillates repeatedly between ℓ_{t+1} and u_{t+1} , so some singular values that are near u_t may get mapped down to ℓ_{t+1} . It so happens that this non-monotonicity—even of a single singular value at a single iteration—causes loss of precision. That is, problems occur if

$$\frac{p_t(\sigma_i)}{\sigma_i} \ll \frac{\max_{x \in [\sigma_{\min}, \sigma_{\max}]} p_t(x)}{\sigma_{\max}},$$

where $0 \leq \sigma_{\min} \leq \sigma_i \leq \sigma_{\max}$ are singular values of \mathbf{X}_t [35]. (In the extreme case, if $p_t(\sigma_i) < 0$, the i th singular vector will change sign and the method will converge to the polar factor of the wrong matrix.) Unlike Newton-Schulz, unscaled Newton, or QDWH, our method is affected by this loss of precision. To mitigate this issue, [12] modify their update polynomials as follows to impose a lower limit on $\frac{p_t(\sigma_i)}{\sigma_i}$. Notice that the issue only occurs when $\ell_t \ll u_t$; as $\ell_t \rightarrow u_t$, our optimal polynomial approaches the Padé approximant and so $\frac{p_t(x)}{x} \geq 1$ for all $x \in [0, u_t]$. We could fully solve the problem by using the Padé approximant instead of our optimal polynomial, but this would significantly slow convergence. Instead we compromise. When $\ell_t \geq u_t/10$, we find that $\frac{p_t(x)}{x} \geq 0.231$. Therefore, whenever $\ell_t < u_t/10$ we select the update rule as though $\ell_t = u_t/10$. This change slows convergence, but only very slightly. (The choice of 10 is somewhat arbitrary. In Appendix G, we use a different factor.)

The third change is copied from the original **Muon** implementation: normalize \mathbf{M} by $\|\mathbf{M}\|_F + 10^{-7}$ instead of by $\|\mathbf{M}\|_F$. As before, we set $u_1 = 1$.

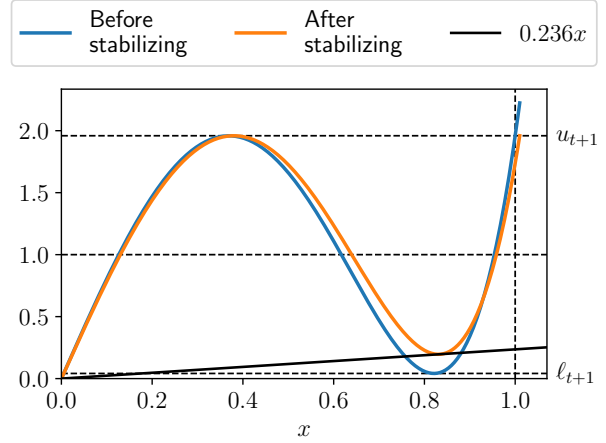


Figure 3: Effects of stabilizing the update rules with a safety factor and cushioning, as described in Section 4.4. The blue curve is the optimal degree-5 polynomial for the interval $[0.005, 1]$. It has numerical issues because it maps singular values near 0.8 down to almost zero and maps $1 + \epsilon$ to $\approx u_{t+1} + 25\epsilon$. The stabilized version is better because it ensures $\frac{p_t(x)}{x} \geq 0.236$ and maps all $x \leq 1.01$ to at most u_{t+1} .

4.5 The algorithm

We give the complete pseudocode for our proposed method in [Algorithm 1](#). Our algorithm first computes the polynomials p_1, \dots, p_T of [Theorem 4.1](#) in full precision using the Remez algorithm. This stage is offline because the coefficients of the polynomials are only computed and stored once. For every subsequent call to the algorithm, these coefficients are reused and the offline stage is skipped. The polynomial $p^* := p_T \circ \dots \circ p_1$ is then applied to the input matrix M in the online stage. The online stage can be performed in lower precision (`bf16`) for greater speed on a GPU.

Algorithm 1 The Polar Express

input: Matrix M , iteration count T , degree d , approximate lower bound ℓ .

output: An approximation X_T to $\text{polar}(M)$.

```

1: Offline stage: ▷ In float64
2:  $\ell_1 = \ell, u_1 = 1.$ 
3: for  $t = 1, 2, \dots, T$  do
4:   Solve using Remez Appendix D:
5:    $p_t = \underset{p \in \mathbb{P}_d^{\text{odd}}}{\text{argmin}} \max_{x \in [\max(\ell_t, u_t/10), u_t]} |1 - p(x)|.$ 
6:    $p_t \leftarrow p_t(\cdot/1.01).$ 
7:    $\ell_{t+1} = p_t(\ell_t), u_{t+1} = 2 - \ell_{t+1}.$ 
8: end for
9: Online stage: ▷ In float16
10: Let  $X_0 = M / (\|M\|_F + 10^{-7}).$ 
11: for  $t = 1, 2, \dots, T$  do
12:    $X_t = p_t(X_{t-1}).$ 
13: end for
14: return  $X_T.$ 

```

Horner's rule can be used to carry out each iteration. For instance, if $p_t = ax + bx^3 + cx^5$, then

$$X_t = X_{t-1} (aI + Y_{t-1} (bI + cY_{t-1}))$$

where $Y_{t-1} = X_{t-1}^\top X_{t-1}$. A simple implementation of the offline stage of [Algorithm 1](#) is given in [Appendix G](#).

For deep learning applications, we recommend using $d = 5$ and $T = 5$ or 6 with $\ell_1 = 10^{-3}$. With these parameters, the offline stage gives the following sequence of polynomials, as generated by the code in [Appendix G](#):

$$\begin{aligned}
p_1(x) &= 8.20516x - 22.90193x^3 + 16.46072x^5 \\
p_2(x) &= 4.06692x - 2.86128x^3 + 0.51838x^5 \\
p_3(x) &= 3.91349x - 2.82425x^3 + 0.52485x^5 \\
p_4(x) &= 3.30601x - 2.43023x^3 + 0.48695x^5 \\
p_5(x) &= 2.30402x - 1.64272x^3 + 0.40091x^5.
\end{aligned} \tag{17}$$

All told, our proposal for Muon is to apply the composition of these polynomials to $M / (\|M\|_F + 10^{-7})$.

5 Numerical experiments

5.1 Convergence of Polar Express

We compare the performance of **Polar Express** against degree-5 Newton-Schulz, and the methods of Chen and Chow, Jordan, and You. We first study an idealized scenario where the spectrum of the input matrix is known exactly. We generate a random matrix whose singular values are evenly spaced on a logarithmic scale between 10^{-6} and 1 . The right and

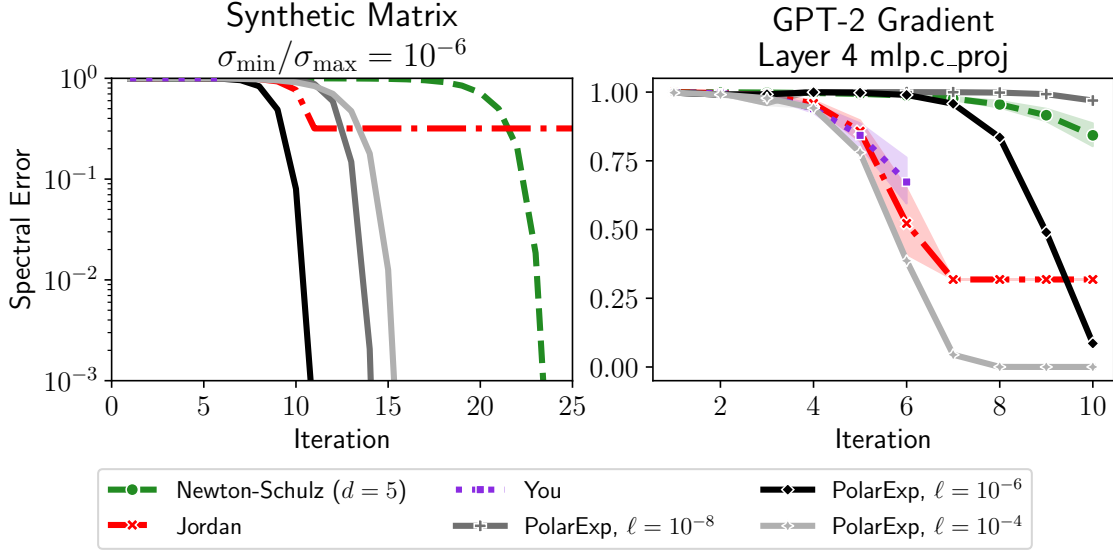


Figure 4: Convergence of various degree-5 polynomial methods in the spectral norm. When tuned properly, Polar Express attains outperforms the other methods at every iteration. Left panel: synthetic matrix with $\sigma_{\max} = 1$, $\sigma_{\min} = 10^{-6}$. Right panel: gradient of a certain weight matrix of a randomly-initialized GPT-2 architecture on a batch of language modeling data, normalized by the Frobenius norm.

left singular vectors are chosen at random. The left panel of Figure 4 shows the results. Since all the methods in this plot use degree-5 polynomials, their computational and runtime costs are all proportional to the number of iterations. As expected, Newton-Schulz converges but makes almost no progress for the first 17 iterations. Jordan’s method achieves error of ≈ 0.3 after just 11 iterations, but ceases to converge further. Your method, which is only defined for six iterations, is barely visible on this plot. When Polar Express is instantiated with $\ell = \sigma_{\min}$, it dominates the other methods at every iteration, achieving excellent accuracy after just 11 iterations and converging about twice as fast as Newton-Schulz to any given error. Even when the lower bound on σ_{\min} is wrong by two orders of magnitude in either direction, the method remains competitive, though it does not actually outperform Keller until iteration 13 or 14.

We next test the methods’ performance on a matrix from a real-world application, namely, the gradient of a weight matrix from the fourth transformer block of a GPT-2 architecture with respect to a language modeling objective on a batch of text from the Tiny Shakespeare dataset [25]. The right panel of Figure 4 shows the results. Once again, the best-tuned version of Polar Express outperforms the other methods. This time, we see that setting ℓ to be many orders of magnitude too small can delay convergence significantly.

For most other weight matrices in this GPT-2 model, the methods all take more than 10 iterations to converge in the spectral norm. The spectral error is be large if there is even one outlying singular value that is far from 1. However, for some applications, we may be satisfied with a weaker notion of convergence, like the relative Frobenius norm. Figure 5 shows the performance of various methods on this metric. We use gradient matrices of the same model, but from two different layers. In addition, we compare the degree-5 methods to Chen and Chow’s degree-3 method. To make this comparison fair, we measure

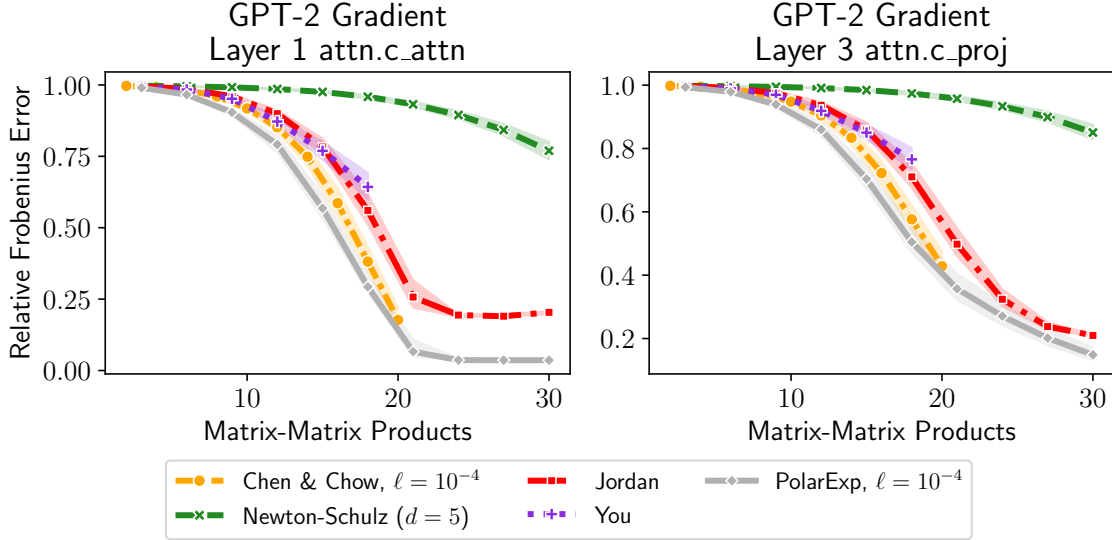


Figure 5: Convergence of polynomial methods in the Frobenius norm on GPT-2 gradient matrices. The number of matrix-matrix products is $T(d+1)/2$, where d is the degree (3 for Chen & Chow; 5 for all others) and T is the number of iterations.

the number of matrix-matrix products performed by each method instead the number of iterations. We find that **Polar Express** can once again dominate the other methods across iterations. Chen and Chow’s method is also quite competitive, and the remaining methods behave much as in Figure 4.

5.2 Training GPT-2

In our final experiment, we compare the performance of using our **Polar Express** method as given in (17) inside the **Muon** algorithm versus Jordan’s [23] and You’s [10] methods.

Our experimental setup is based on the modified **nanogpt** code of Jordan [22]. We train a GPT-2 model with $n_{\text{embd}} = 768$, $n_{\text{layer}} = 12$, $n_{\text{head}} = 12$, and a vocabulary size of 50,257, using a context length of 1024. Training is performed on 1B tokens from the FINEWEB dataset [3], using a batch size of 32 and a single epoch. All models are trained with mixed precision (**bfloat16**) on 4 H100 GPUs. For all methods we use the learning rate schedule proposed in [22], consisting of a constant phase for the first 40% of training steps followed by a linear decay. All methods for the matrix sign computations are performed in **float16b** precision and use five iterations.

Figure 6 shows the resulting runs of each method in terms of validation loss and training loss, where we can see that **muon-PolarExp**, achieves better validation and training loss than **muon-Jordan** or **muon-You**. Since each iteration of the different matrix sign methods are equally expensive (since they all apply a degree 5 polynomial), improved validation loss in terms of epochs also translates to an improved loss in terms of wall clock time (see bottom right of Figure 6). The advantage is remarkably consistent across all learning rates and epochs.

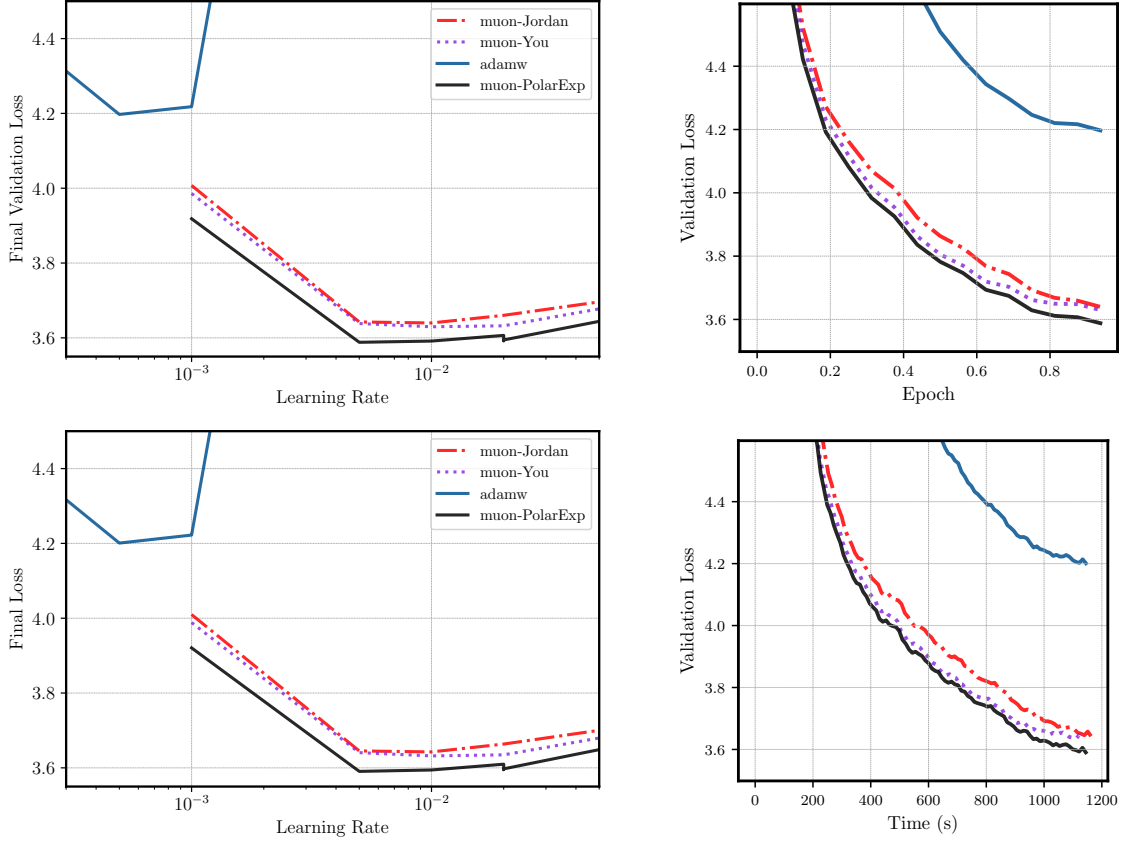


Figure 6: Training a GPT-2 (124M) model on 1 Billion tokens of the Fineweb data set [3]. The Legend muon-**<name>** refers to using muon with the **<name>** method for computing polar(M). Top Left: The final validation loss vs. the learning rate. The final best validation losses for each method were, in reverse order, **adamw**: 4.197, **muon-Jordan**: 3.639, **muon-You**: 3.629 and **muon-PolarExp**: 3.588. Bottom Left: The final training loss vs the learning rate. Top Right: Validation loss vs. number of iterations. Bottom Left: validation loss vs. time, plotting each method with its best learning rate.

References

- [1] N. I. Achieser. *Theory of approximation*. Dover Publications, Inc., New York, 1992. Translated from the Russian and with a preface by Charles J. Hyman, Reprint of the 1956 English translation.
- [2] Rohan Anil, Vineet Gupta, Tomer Koren, Kevin Regan, and Yoram Singer. Scalable second order optimization for deep learning. *arXiv preprint arXiv:2002.09018*, 2020. URL: <https://arxiv.org/abs/2002.09018>.
- [3] Samuel Aroca-Ouellette, Philippe Beaudoin, Guillaume Lajoie, Liam Paull, Joelle Pineau, Pascal Vincent, and Anirudh Goyal. Fineweb: Learning language models with high quality web data. In *NeurIPS Datasets and Benchmarks Track*, 2023. URL: <https://arxiv.org/abs/2306.03061>.

- [4] Michele Benzi and Ru Huang. Some matrix properties preserved by generalized matrix functions. *Spec. Matrices*, 7:27–37, 2019. doi:[10.1515/spma-2019-0003](https://doi.org/10.1515/spma-2019-0003).
- [5] Jeremy Bernstein and Laker Newhouse. Modular duality in deep learning. *arXiv preprint arXiv:2410.21265*, 2024. URL: <https://arxiv.org/abs/2410.21265>.
- [6] Jeremy Bernstein and Laker Newhouse. Old optimizer, new norm: An anthology. *arXiv preprint arXiv:2409.20325*, 2024. URL: <https://arxiv.org/abs/2409.20325>.
- [7] Å. Björck and C. Bowie. An iterative algorithm for computing the best estimate of an orthogonal matrix. *SIAM J. Numer. Anal.*, 8:358–364, 1971. doi:[10.1137/0708036](https://doi.org/10.1137/0708036).
- [8] Christos Boutsikas, Petros Drineas, and Ilse C. F. Ipsen. Small singular values can increase in lower precision. *SIAM J. Matrix Anal. Appl.*, 45(3):1518–1540, 2024. doi:[10.1137/23M1557209](https://doi.org/10.1137/23M1557209).
- [9] J Douglas Carroll and Phipps Arabie. Multidimensional scaling. pages 179–250, 1998. URL: <https://www.sciencedirect.com/science/article/pii/B9780120999750500051>, doi:[10.1016/B978-012099975-0.50005-1](https://doi.org/10.1016/B978-012099975-0.50005-1).
- [10] Franz Louis Cesista, You Jiacheng, and Keller Jordan. Squeezing 1-2% efficiency gains out of muon by optimizing the newton-schulz coefficients, 2025. URL: <http://leloykun.github.io/ponder/muon-opt-coeffs/>.
- [11] PL Chebyshev. Questions on smallest quantities connected with the approximate representation of functions (1859). *Collected works*, 2:151–235, 1947.
- [12] Jie Chen and Edmond Chow. A stable scaling of newton-schulz for improving the sign function computation of a hermitian matrix. *Preprint ANL/MCS-P5059-0114*, 2014. URL: <https://www.mcs.anl.gov/papers/P5059-0114.pdf>.
- [13] E. W. Cheney. *Introduction to approximation theory*. McGraw-Hill Book Co., New York-Toronto-London, 1966.
- [14] John Duchi, Elad Hazan, and Yoram Singer. Adaptive subgradient methods for online learning and stochastic optimization. *J. Mach. Learn. Res.*, 12:2121–2159, 2011.
- [15] Alexandre Eremenko and Peter Yuditskii. Uniform approximation of $\operatorname{sgn} x$ by polynomials and entire functions. *J. Anal. Math.*, 101:313–324, 2007. doi:[10.1007/s11854-007-0011-3](https://doi.org/10.1007/s11854-007-0011-3).
- [16] Gene H. Golub and Charles F. Van Loan. *Matrix computations*. Johns Hopkins Studies in the Mathematical Sciences. Johns Hopkins University Press, Baltimore, MD, fourth edition, 2013.
- [17] J. C. Gower and G. B. Dijksterhuis. *Procrustes problems*, volume 30 of *Oxford Statistical Science Series*. Oxford University Press, Oxford, 2004. doi:[10.1093/acprof:oso/9780198510581.001.0001](https://doi.org/10.1093/acprof:oso/9780198510581.001.0001).
- [18] Vineet Gupta, Tomer Koren, and Yoram Singer. Shampoo: Preconditioned stochastic tensor optimization. In Jennifer Dy and Andreas Krause, editors, *Proceedings of the 35th International Conference on Machine Learning*, volume 80 of *Proceedings of Machine Learning Research*, pages 1842–1850. PMLR, 10–15 Jul 2018. URL: <https://proceedings.mlr.press/v80/gupta18a.html>.

- [19] Nicholas J. Higham. Computing the polar decomposition—with applications. *SIAM J. Sci. Statist. Comput.*, 7(4):1160–1174, 1986. doi:[10.1137/0907079](https://doi.org/10.1137/0907079).
- [20] Nicholas J. Higham. *Functions of matrices*. SIAM, Philadelphia, PA, 2008. doi:[10.1137/1.9780898717778](https://doi.org/10.1137/1.9780898717778).
- [21] Elias Jarlebring and Gustaf Lorentzon. The polynomial set associated with a fixed number of matrix-matrix multiplications. *arXiv preprint arXiv:2504.01500*, 2025. URL: <https://arxiv.org/abs/2504.01500>.
- [22] Keller Jordan, Jeremy Bernstein, Brendan Rappazzo, @fernbear.bsky.social, Boza Vlado, You Jiacheng, Franz Cesista, Braden Koszarsky, and @Grad62304977. modded-nanogpt: Speedrunning the nanogpt baseline, 2024. URL: <https://github.com/KellerJordan/modded-nanogpt>.
- [23] Keller Jordan, Yuchen Jin, Vlado Boza, Jiacheng You, Franz Cesista, Laker Newhouse, and Jeremy Bernstein. Muon: An optimizer for hidden layers in neural networks, 2024. URL: <https://kellerjordan.github.io/posts/muon/>.
- [24] Tetsuya Kaneko, Simone Fiori, and Toshihisa Tanaka. Empirical arithmetic averaging over the compact Stiefel manifold. *IEEE Trans. Signal Process.*, 61(4):883–894, 2013. doi:[10.1109/TSP.2012.2226167](https://doi.org/10.1109/TSP.2012.2226167).
- [25] Andrej Karpathy. char-rnn. <https://github.com/karpathy/char-rnn>, 2015.
- [26] Charles Kenney and Alan J. Laub. Rational iterative methods for the matrix sign function. *SIAM J. Matrix Anal. Appl.*, 12(2):273–291, 1991. doi:[10.1137/0612020](https://doi.org/10.1137/0612020).
- [27] Diederik P. Kingma and Jimmy Ba. Adam: A method for stochastic optimization. In *International Conference on Learning Representations*, 2015. URL: <http://arxiv.org/abs/1412.6980>.
- [28] Zdislav Kovářík. Some iterative methods for improving orthonormality. *SIAM J. Numer. Anal.*, 7:386–389, 1970. doi:[10.1137/0707031](https://doi.org/10.1137/0707031).
- [29] Eunsang Lee, Joon-Woo Lee, Jong-Seon No, and Young-Sik Kim. Minimax approximation of sign function by composite polynomial for homomorphic comparison. *IEEE Transactions on Dependable and Secure Computing*, 19(6):3711–3727, 2022. doi:[10.1109/TDSC.2021.3105111](https://doi.org/10.1109/TDSC.2021.3105111).
- [30] R. B. Leipnik. Rapidly convergent recursive solution of quadratic operator equations. *Numer. Math.*, 17:1–16, 1971. doi:[10.1007/BF01395861](https://doi.org/10.1007/BF01395861).
- [31] Jingyuan Liu, Jianlin Su, Xingcheng Yao, Zhejun Jiang, Guokun Lai, Yulun Du, Yidao Qin, Weixin Xu, Enzhe Lu, Junjie Yan, et al. Muon is scalable for LLM training. *arXiv preprint arXiv:2502.16982*, 2025. URL: <https://arxiv.org/abs/2502.16982>.
- [32] Ilya Loshchilov and Frank Hutter. Decoupled weight decay regularization. In *International Conference on Learning Representations*, 2019. URL: <https://openreview.net/forum?id=Bkg6RiCqY7>.
- [33] Yuji Nakatsukasa, Zhaojun Bai, and François Gygi. Optimizing Halley’s iteration for computing the matrix polar decomposition. *SIAM J. Matrix Anal. Appl.*, 31(5):2700–2720, 2010. doi:[10.1137/090774999](https://doi.org/10.1137/090774999).

- [34] Yuji Nakatsukasa and Roland W. Freund. Computing fundamental matrix decompositions accurately via the matrix sign function in two iterations: the power of Zolotarev’s functions. *SIAM Rev.*, 58(3):461–493, 2016. doi:[10.1137/140990334](https://doi.org/10.1137/140990334).
- [35] Yuji Nakatsukasa and Nicholas J. Higham. Backward stability of iterations for computing the polar decomposition. *SIAM J. Matrix Anal. Appl.*, 33(2):460–479, 2012. doi:[10.1137/110857544](https://doi.org/10.1137/110857544).
- [36] Yuji Nakatsukasa and Nicholas J. Higham. Stable and efficient spectral divide and conquer algorithms for the symmetric eigenvalue decomposition and the SVD. *SIAM J. Sci. Comput.*, 35(3):A1325–A1349, 2013. doi:[10.1137/120876605](https://doi.org/10.1137/120876605).
- [37] Herbert Neuberger. Exactly massless quarks on the lattice. *Phys. Lett. B*, 417(1-2):141–144, 1998. doi:[10.1016/S0370-2693\(97\)01368-3](https://doi.org/10.1016/S0370-2693(97)01368-3).
- [38] Ricardo Pachón and Lloyd N. Trefethen. Barycentric-Remez algorithms for best polynomial approximation in the chebfun system. *BIT*, 49(4):721–741, 2009. doi:[10.1007/s10543-009-0240-1](https://doi.org/10.1007/s10543-009-0240-1).
- [39] T Parks and James McClellan. Chebyshev approximation for nonrecursive digital filters with linear phase. *IEEE Transactions on circuit theory*, 19(2):189–194, 1972. doi:[10.1109/TCT.1972.1083419](https://doi.org/10.1109/TCT.1972.1083419).
- [40] Michael S. Paterson and Larry J. Stockmeyer. On the number of nonscalar multiplications necessary to evaluate polynomials. *SIAM J. Comput.*, 2:60–66, 1973. doi:[10.1137/0202007](https://doi.org/10.1137/0202007).
- [41] Ishaan Shah, Anthony M Polloreno, Karl Stratos, Philip Monk, Adarsh Chaluvvaraju, Andrew Hojel, Andrew Ma, Anil Thomas, Ashish Tanwer, Darsh J Shah, et al. Practical efficiency of muon for pretraining. *arXiv preprint arXiv:2505.02222*, 2025. URL: <https://arxiv.org/abs/2505.02222>.
- [42] Hao-Jun Michael Shi, Tsung-Hsien Lee, Shintaro Iwasaki, Jose Gallego-Posada, Zhijing Li, Kaushik Rangadurai, Dheevatsa Mudigere, and Michael Rabbat. A distributed data-parallel PyTorch implementation of the distributed Shampoo optimizer for training neural networks at-scale. *arXiv preprint arXiv:2309.06497*, 2023. URL: <https://arxiv.org/abs/2309.06497>.
- [43] Modula Systems. Newton-schulz algorithm — jiacheng’s six-step method. <https://docs.modula.systems/algorithms/newton-schulz/#jiacheng-s-six-step>, 2024. Accessed: 2025-05-19.
- [44] Attila Szabo and Neil S Ostlund. *Modern quantum chemistry: introduction to advanced electronic structure theory*. Courier Corporation, 1996.
- [45] Lloyd N. Trefethen. *Approximation theory and approximation practice*. Society for Industrial and Applied Mathematics (SIAM), Philadelphia, PA, extended edition, 2020.
- [46] Greg Yang, James B. Simon, and Jeremy Bernstein. A spectral condition for feature learning, 2024. URL: <https://arxiv.org/abs/2310.17813>, arXiv:2310.17813.

- [47] Zhenyue Zhang, Hongyuan Zha, and Wenlong Ying. Fast parallelizable methods for computing invariant subspaces of Hermitian matrices. *J. Comput. Math.*, 25(5):583–594, 2007. URL: <http://www.jstor.org/stable/43693395>.

A Proof of Theorem 4.1

The aim of this section is to prove Theorem 4.1. We begin with a result that provides a few essential properties for the polynomial solving (8) when $T = 1$. This result is known as Chebyshev’s theorem [11] or the equioscillation theorem [45, Chapter 10].

Lemma A.1. Let $d = 2q + 1$ and $u, \ell > 0$. Consider the problem

$$\min_{p \in \mathbb{P}_d^{\text{odd}}} \max_{x \in [\ell, u]} |1 - p(x)|. \quad (18)$$

There exists a unique polynomial $p^* \in \mathbb{P}_d^{\text{odd}}$ solving (18). Furthermore, p^* is the unique solution to the above problem if and only if there exist $q + 2$ distinct points $\{x_0, \dots, x_{q+1}\} \subset [\ell, u]$ such that

$$1 - p^*(x_i) = \eta(-1)^i \max_{x \in [\ell, u]} |1 - p^*(x)|, \quad \text{for } i = 0, \dots, q + 1,$$

for $\eta = 1$ or $\eta = -1$.

Proof. A discussion can be found in [15]. Here we include a formal proof for completeness.

By Chebyshev’s Theorem [1, 11, 13] it is sufficient to show that $\mathbb{P}_d^{\text{odd}}$ satisfies the Haar condition: any non-zero $p \in \mathbb{P}_d^{\text{odd}} = \text{span}\{x, \dots, x^3, \dots, x^{2q+1}\}$ can have at most q roots in $[\ell, u]$.

Since $\deg(p) = d = 2q + 1$ we know that p can have at most $2q + 1$ roots in \mathbb{R} . However, since $p(0) = 0$ and $p(x) = -p(-x)$ we know that p has one root at zero, and the remaining roots come in symmetric pairs $(x, -x)$. Because of this, p can have at most q roots in the positive orthant, and thus it can have at most q roots in $[\ell, u] \subset (0, \infty)$. Hence, $\mathbb{P}_d^{\text{odd}}$ satisfies the Haar condition, which yields the desired result. \square

The proof of Theorem 4.1 will be by induction on T . We begin by establishing the base case, $T = 1$, which is handled by the following result.

Lemma A.2. Let $u, \ell > 0$ and define

$$p^* := \operatorname{argmin}_{p \in \mathbb{P}_d^*} \max_{x \in [\ell, u]} |1 - p(x)|.$$

Then

$$p^*(\ell) = \min_{x \in [\ell, u]} p^*(x), \quad \max_{x \in [\ell, u]} p^*(x) = 2 - p^*(\ell), \quad \text{and} \quad \max_{x \in [\ell, u]} |1 - p^*(x)| = 1 - p^*(\ell).$$

Proof. Throughout the proof we assume $d = 2q + 1$. We begin with proving

$$p^*(\ell) = \min_{x \in [\ell, u]} p^*(x).$$

Consider the polynomial $e(x) := 1 - p^*(x)$. The proof will contain three steps. We first rule out the trivial case that $p^* \neq 0$, since $p(x) = \frac{2}{\ell+u}x$ would then be a better approximation. Hence, p^* cannot be the zero polynomial.

Step 1: $e(x)$ has exactly q stationary points inside the open interval (ℓ, u) .

Note that $e(x)$ has at most $2q$ stationary points in \mathbb{R} , since its derivative $e'(x)$ is a polynomial of degree $2q$. Furthermore, since p^* is odd, we have that $e'(x) = -p'(x)$ is even of degree $2q$, and thus can have at most q stationary points contained in $(0, +\infty)$. Hence, there can be at most q stationary points of $e(x)$ inside the interval $[\ell, u]$.

By Lemma A.1 there are $q + 2$ points $x_0, \dots, x_{q+1} \in [\ell, u]$ where $e(x)$ is maximized or minimized in $[\ell, u]$. These points are either stationary points or they are endpoints of the interval $[\ell, u]$. Let n_{ext} be the number of stationary points and n_{stat} be the number of endpoints in the set $\{x_0, \dots, x_{q+1}\}$. Since a point can be both a stationary point and an endpoint we have $q + 2 \leq n_{\text{end}} + n_{\text{stat}}$. However, $n_{\text{end}} \leq 2$ and $n_{\text{stat}} \leq q$, which follows from the previous paragraph where we showed that there are at most q stationary points of $e(x)$ in $[\ell, u]$. So $n_{\text{end}} + n_{\text{stat}} \leq q + 2$, and consequently we must have $n_{\text{end}} = 2$ and $n_{\text{stat}} = q$, as required.

Step 2: $x = \ell$ is a maximum of $e(x)$ on the interval $[\ell, u]$

By Lemma A.1 and the discussion from Step 1, we know that $|e(x)|$ is maximized at $q + 2$ points inside $[\ell, u]$ and q of these points are contained inside the open interval (ℓ, u) . Hence, $x = \ell$ must either be a maximum or a minimum of $e(x)$. We will show that $x = \ell$ must be a maximum by contradiction.

Suppose $x = \ell$ was a minimum of $e(x)$ on $[\ell, u]$. First note that p^* is trivially non-negative on $[\ell, u]$, or else $p(x) = 0$ would be a better polynomial. Hence, since $p^*(0) = 0$ we must have $p^{*\prime}(\delta) > 0$ for some $\delta \in [0, \ell]$, or else the zero polynomial $p(x) = 0$ would be a better approximation. Hence, for some $\delta \in [0, \ell]$ we have $e'(\delta) < 0$.

We must also have $e'(\ell) \geq 0$ or else $x = \ell$ is not a minimum of $e(x)$. Since $e'(\delta) < 0$ for some $\delta \in [0, \ell]$ and $e'(\ell) \geq 0$, by the intermediate value theorem there exists a point $x^* \in [0, \ell]$ such that $e'(x^*) = 0$. However, by the discussion above we know that all stationary points of e are contained inside the open interval (ℓ, u) . Hence, $x = \ell$ cannot be a minimum of $e(x)$ on $[\ell, u]$. However, by Step 1 we know that the endpoints of $[\ell, u]$ must be either minima or maxima of $e(x)$. Hence, $x = \ell$ is a maximum of $e(x)$ on $[\ell, u]$.

Step 3: Obtaining the desired equalities

Since $e(x)$ has a maximum in $[\ell, u]$ at $x = \ell$, we have $p^*(\ell) = \min_{x \in [\ell, u]} p^*(x)$. The other two equalities are immediate consequences of the equioscillation property of p^* Lemma A.1 and that $x = \ell$ is a minimum of p^* over the set $[\ell, u]$. \square

With the above-mentioned result in hand, we are ready to prove Theorem 4.1.

Theorem 4.1. Let d be odd and define $\ell_1 = \ell$ and $u_1 = u$. For $t = 1, \dots, T$ define

$$\begin{aligned} p_t &= \operatorname{argmin}_{p \in \mathbb{P}_d^{\text{odd}}} \max_{x \in [\ell_t, u_t]} |1 - p(x)| \\ \ell_{t+1} &= \min_{x \in [\ell_t, u_t]} p_t(x) \\ u_{t+1} &= \max_{x \in [\ell_t, u_t]} p_t(x) \end{aligned} \tag{10}$$

Then the new error, lower and upper bounds can be computed through

$$\ell_{t+1} = p_t(\ell_t), \quad u_{t+1} = 2 - \ell_{t+1}, \quad \text{and} \quad \max_{x \in [\ell_t, u_t]} |1 - p_t(x)| = 1 - \ell_{t+1}. \quad (11)$$

Furthermore, the composition $p^* := p_T \circ p_{T-1} \circ \cdots \circ p_1$ is optimal and the error is given by:

$$\max_{x \in [\ell, u]} |1 - p^*(x)| = \min_{\substack{p = p_T \circ p_{T-1} \circ \cdots \circ p_1 \\ p_t \in \mathbb{P}_d^{\text{odd}}}} \max_{x \in [\ell, u]} |1 - p(x)| = 1 - \ell_{T+1}. \quad (12)$$

Proof. The proof of (11) is an immediate consequence of Lemma A.2, since for each $t = 1, \dots, T$, p_t is the optimal approximation in $\mathbb{P}_d^{\text{odd}}$ to $x \mapsto 1$.

We now proceed with the proof of (12), which will be by induction. The proof for $T = 1$ is an immediate consequence of Lemma A.2 and we also have $p^*(\ell) = \ell_2$ by (11). Now suppose the result is true for all $t \leq T - 1$. For $t = 1, \dots, T - 1$, note that the image of p_t on $[\ell_t, u_t]$ is exactly $[\ell_{t+1}, u_{t+1}]$ by i). Hence, if we define $g(x) := p_{T-1} \circ \cdots \circ p_1(x)$, then the image of g on $[\ell, u]$ is $[\ell_T, u_T]$. Furthermore, by i) we also have $g(\ell) = \ell_T$. Pick any f such that $f \neq g$ and

$$f = \tilde{p}_{T-1} \circ \cdots \circ \tilde{p}_1,$$

for some $\tilde{p}_1, \dots, \tilde{p}_{T-1} \in \mathbb{P}_d^{\text{odd}}$. Let the image of f on $[\ell, u]$ be $[a, b]$. We will prove that $\frac{a}{b} \leq \frac{\ell_T}{u_T}$ by contradiction.

Suppose $\frac{a}{b} > \frac{\ell_T}{u_T}$. Define $c = \frac{2}{a+b}$. Then, the image of the scaled function cf on $[\ell, u]$ is $[ca, cb]$ and cf satisfies

$$\max_{x \in [\ell, u]} |1 - cf(x)| = \max \{1 - ca, cb - 1\} = \frac{b - a}{a + b}.$$

Recall by our inductive hypothesis, we have $\max_{x \in [\ell, u]} |1 - g(x)| = 1 - \ell_T = u_T - 1$ where the second equality holds by (11). It follows that

$$\begin{aligned} \frac{a}{b} &> \frac{\ell_T}{u_T} \\ \Leftrightarrow \frac{a}{b} &> \frac{\ell_T}{2 - \ell_T} \\ \Leftrightarrow \ell_T &< \frac{2a}{a + b} \\ \Leftrightarrow 1 - \ell_T &> \frac{b - a}{a + b} \\ \Leftrightarrow \max_{x \in [\ell, u]} |1 - g(x)| &> \max_{x \in [\ell, u]} |1 - cf(x)|, \end{aligned}$$

which leads to a contradiction to our inductive hypothesis that g is optimal. Hence, we must have $\frac{a}{b} \leq \frac{\ell_T}{u_T}$.

Consequently, using that $\frac{a}{b} \leq \frac{\ell_T}{u_T}$, we will show that for any $\tilde{p}_T \in \mathbb{P}_d^{\text{odd}}$ and for any $f = \tilde{p}_{T-1} \circ \cdots \circ \tilde{p}_1$ $\tilde{p}_T \circ f$ cannot be a better approximation than $p_T \circ g$. In particular, we have

$$\begin{aligned}
\max_{x \in [\ell, u]} |1 - \tilde{p}_T(f(x))| &\geq \min_{p \in \mathbb{P}_d^*} \max_{x \in [\ell, u]} |1 - p(f(x))| \\
&= \min_{p \in \mathbb{P}_d^*} \max_{x \in [a, b]} |1 - p(x)| \\
&= \min_{p \in \mathbb{P}_d^*} \max_{x \in [a/b, 1]} |1 - p(x)| \\
&\geq \min_{p \in \mathbb{P}_d^*} \max_{x \in [\ell_T/u_T, 1]} |1 - p(x)| \\
&= \min_{p \in \mathbb{P}_d^*} \max_{x \in [\ell_T, u_T]} |1 - p(x)| \\
&= \min_{p \in \mathbb{P}_d^*} \max_{x \in [\ell, u]} |1 - p(g(x))| \\
&= \max_{x \in [\ell_T, u_T]} |1 - p_T(g(x))| = 1 - p_T(\ell_T) = 1 - \ell_{T+1},
\end{aligned}$$

where the second and third equality follow by changing variables $y = x/b$ so that

$$\min_{p \in \mathbb{P}_d^*} \max_{x \in [a, b]} |1 - p(x)| = \min_{p \in \mathbb{P}_d^*} \max_{y \in [a/b, 1]} |1 - p(by)| = \min_{p \in \mathbb{P}_d^*} \max_{y \in [a/b, 1]} |1 - p(y)|$$

and this last equality follows because the space \mathbb{P}_d^* is invariant under input rescaling; that is, for any $b \neq 0$, the map $x \mapsto bx$ preserves the space $\text{span}\{x, x^3, \dots, x^d\}$. This concludes the proof. \square

B Proof of Theorem 4.3

In this section we provide the proof of the convergence guarantee stated in [Theorem 4.3](#).

Theorem 4.3. Let \mathbf{M} be a matrix normalized so that $\sigma(\mathbf{M}) \subset [\ell, 1]$. Let $\mathbf{X}_T = p^*(\mathbf{M})$, where p^* is the polynomial from [Theorem 4.1](#) with $d = 2q + 1$. Then, we have

$$\|\text{polar}(\mathbf{M}) - \mathbf{X}_T\|_2 \leq |1 - \ell^2|^{(q+1)^T}. \quad (14)$$

Hence, for $d = 3$ the method converges quadratically and for $d = 5$ the method converges cubically.

Proof. Define

$$p^* = \underset{\substack{p = p_T \circ p_{T-1} \circ \dots \circ p_1 \\ p_t \in \mathbb{P}_d^*}}{\text{argmin}} \max_{x \in [\ell, u]} |1 - p(x)|.$$

Then [Algorithm 1](#) returns $\mathbf{X}_T = p^*(\mathbf{M})$. Let $h \in \mathbb{P}_q$ be $[q/0]$ Padé-approximant to $(1-x)^{-1/2}$ [26, Section 3] and define $p(x) = xh(1-x^2) \in \mathbb{P}_d^{\text{odd}}$. Define $f = p \circ \dots \circ p$ as the composition of p with itself T times. Then, by [Theorem 4.1](#) and [26, Theorem 3.1] we have

$$\begin{aligned}
\|\text{sign}(\mathbf{M}) - \mathbf{X}_T\|_2 &\leq \max_{x \in [\ell, 1]} |1 - p^*(x)| \\
&\leq \max_{x \in [\ell, 1]} |1 - f(x)| \\
&\leq \max_{x \in [\ell, 1]} \left[\frac{|1 - x^2|^{(d+1)^T}}{1 + f(x)} \right] \\
&\leq |1 - \ell^2|^{(d+1)^T},
\end{aligned}$$

as required. \square

C Proof of equivalence between (7) and (8)

In this section we provide a proof for the equivalence between (7) and (8). It is sufficient to show that for any fixed polynomial p we have

$$\varepsilon_1 := \max_{\substack{\mathbf{M} \in \mathbb{R}^{m \times n} \\ \sigma(\mathbf{M}) \subset [\ell, u]}} \|\text{polar}(\mathbf{M}) - p(\mathbf{M})\|_2 = \max_{x \in [\ell, u]} |1 - p(x)| := \varepsilon_2.$$

For any fixed \mathbf{M} , by the unitary invariance of the spectral norm we immediately have

$$\|\text{polar}(\mathbf{M}) - p(\mathbf{M})\|_2 = \max_{\sigma_i \in \sigma(\mathbf{M})} |1 - p(\sigma_i)| \leq \max_{x \in [\ell, u]} |1 - p(x)|.$$

Consequently, $\varepsilon_1 \leq \varepsilon_2$.

Suppose that $x^* \in [\ell, u]$ is chosen so that $|1 - p(x^*)| = \max_{x \in [\ell, u]} |1 - p(x)|$. Without loss of generality, assume $m \geq n$. Letting $\mathbf{M} = x^* \mathbf{U} \mathbf{V}^\top$, for any matrix $\mathbf{U} \in \mathbb{R}^{m \times n}$ and $\mathbf{V} \in \mathbb{R}^{n \times n}$ with orthonormal columns, and noting $\text{polar}(\mathbf{M}) = \mathbf{U} \mathbf{V}^\top$ yields

$$\begin{aligned} \|\text{polar}(\mathbf{M}) - p(\mathbf{M})\|_2 &= \|\mathbf{I}_n - p(x^*) \mathbf{I}_n\|_2 \\ &= |1 - p(x^*)| \\ &= \max_{x \in [\ell, u]} |1 - p(x)|. \end{aligned}$$

Consequently, $\varepsilon_1 \geq \varepsilon$. Hence, $\varepsilon_1 = \varepsilon_2$, as desired.

D Remez algorithm

[Theorem 4.1](#) shows that we can solve (8) by greedily choosing the optimal approximation $p_t \in \mathbb{P}_d^{\text{odd}}$ for each interval $[\ell_t, u_t]$ for $t = 1, \dots, T$. In this section, we outline how the Remez algorithm [38, 39] can be used to approximate p_t .

We begin with the case when $d = 3$. In this case, there is a simple closed form for the optimal odd polynomial $p^* \in \mathbb{P}_3^{\text{odd}}$; see [12]. On a given interval $[\ell, u]$, the optimal approximation to the constant function $x \mapsto 1$ is given by the scaled and shifted Newton-Schulz polynomial $p_{\text{NS}}(x) = \frac{3}{2}x - \frac{1}{2}x^3$:

$$p^*(x) = \beta p_{\text{NS}}(\alpha x), \text{ where } \alpha = \sqrt{\frac{3}{u^2 + lu + \ell^2}} \text{ and } \beta = \frac{4}{2 + \ell u(\ell + u)\alpha^3}.$$

One can verify that this polynomial satisfies the equioscillation condition from [Lemma A.1](#) at $x = \ell, \frac{1}{\alpha}, u$ and therefore necessarily has to be the optimal approximation from $\mathbb{P}_3^{\text{odd}}$. Unfortunately, for larger d finding closed form expressions for optimal approximations from $\mathbb{P}_d^{\text{odd}}$ becomes challenging. In fact, to the best of our knowledge the optimal approximation is not known for $d \geq 5$. However, we can approximate the optimal polynomial using the Remez algorithm.

Let $d = 2q + 1$. Recall that from [Lemma A.1](#) the optimal polynomial must satisfy the equioscillation property $q + 2$ times. The Remez algorithm is an iterative algorithm that finds the equioscillation points $A = \{x_0, \dots, x_{q+1}\}$ from [Lemma A.1](#) by iteratively refining

a sequence of trial points $A^{(k)} = \{x_0^{(k)}, \dots, x_{q+1}^{(k)}\}$ so that $A^{(k)}$ converges to A . From the sequence of trial points $A^{(k)}$ the algorithm also finds a sequence of polynomials $p^{(k)}$ so that $p^{(k)}$ converges to the optimal polynomial. The convergence is extremely fast, and usually 10 iterations is sufficient to converge to the optimal polynomial up to double precision machine epsilon [38]. More commonly, the Remez algorithm is used to find optimal polynomial approximations to general continuous functions where $d \approx 100$ or even $d \approx 1000$. However, because the polynomial we build to approximate $\text{sign}(x)$ is a composition of polynomials, each of which has a low degree, in our setting the degree d is small, usually $d = 5$. For $d = 5$ the Remez algorithm admits a simple description, as we outline below. The following description can be generalized to arbitrary d .

Recall that as stated in Lemma A.1, the unique optimal approximation $p^* \in \mathbb{P}_5^{\text{odd}}$ satisfies the equioscillation property four times. The Remez algorithm first starts with a trial set $A^{(1)} = \{x_0^{(1)}, x_1^{(1)}, x_2^{(1)}, x_3^{(1)}\} \subset [\ell, u]$ which *ideally* should approximately satisfy the equioscillation property. Since we know that ℓ and u must be equioscillation points we always set $x_0^{(k)} = \ell$ and $x_3^{(k)} = u$ for all k . $x_2^{(1)}$ and $x_3^{(1)}$ are chosen equispaced to be $\frac{1}{4}\ell + \frac{3}{4}u$ and $\frac{3}{4}\ell + \frac{1}{4}u$, since we observe that as $\ell \approx u$ these are approximately the equioscillation points. Next, the algorithm solves the following system of equations

$$a_1 x_i^{(1)} + b_1 (x_i^{(1)})^3 + c_1 (x_i^{(1)})^5 + (-1)^i E_1 = \text{sign}(x) = 1, \quad i = 0, 1, 2, 3, \quad (19)$$

for the unknowns a_1, b_1, c_1 , and E_1 . Recalling that $x_0^{(1)} = \ell$ and $x_3^{(1)} = u$, (19) can equivalently be written as a system of linear equations

$$\begin{bmatrix} \ell & \ell^3 & \ell^5 & 1 \\ x_1^{(1)} & (x_1^{(1)})^3 & (x_1^{(1)})^5 & -1 \\ x_2^{(1)} & (x_2^{(1)})^3 & (x_2^{(1)})^5 & 1 \\ u & u^3 & u^5 & -1 \end{bmatrix} \begin{bmatrix} a \\ b \\ c \\ E \end{bmatrix} = \begin{bmatrix} 1 \\ 1 \\ 1 \\ 1 \end{bmatrix}. \quad (20)$$

Once we have solved for a_1, b_1, c_1 , and E_1 we set $p^{(k)}(x) = a_1 x + b_1 x^3 + c_1 x^5$. Now we want to find the worst case error of using $p^{(k)}$ to approximate $x \mapsto 1$. We therefore find local maxima of the error function $e_1(x) = 1 - p_1(x)$ on (ℓ, u) by setting the derivative of $e_1(x)$ to zero and solving for x . This results in solving a quadratic equation $5b_1 x^4 + 3b_1 x^2 + a = 0$, which have closed form solutions from the quadratic formula. We now let $x_1^{(2)}$ and $x_2^{(2)}$ be the solutions to this equation and let $A^{(2)} = \{\ell, x_1^{(2)}, x_2^{(2)}, u\}$ and repeat the procedure until $|E_k| := \max_{x \in [\ell, u]} |1 - p^{(k)}(x)| \approx \max_{x \in [\ell, u]} |1 - p^{(k+1)}(x)| := |E_{k+1}|$.

We emphasize that the matrix appearing in (20) is a Vandermonde matrix, which become notoriously ill-conditioned as d grows large [16, Section 4.6]. However, since in our setting we allow d to be small there is no ill-conditioning due to the size of the matrix. Instead, we observe ill-conditioning when $\ell \approx u$. However, as $\ell/u \rightarrow 1$ the optimal polynomial will converge to the polynomial $\frac{x/u}{8} (15 - 10(x/u)^2 + 3(x/u)^4)$, which can be verified by noting that as $\ell/u \rightarrow 1$ all equioscillation points x_0, x_1, x_2, x_3 must converge to u . For general $d = 2q + 1$, the polynomial will converge to $(x/\ell)h(1 - (x/\ell)^2)$ where $h \in \mathbb{P}_q$ is the $[q/0]$ Padé approximant to $(1 - x)^{1/2}$ [26]. In fact, this polynomial is extremely close to the optimal polynomial for sufficiently large ℓ . To see this, let p^* be the optimal

approximation from $\mathbb{P}_5^{\text{odd}}$ and let $p(x) = \frac{x/u}{8} (15 - 10(x/u)^2 + 3(x/u)^4)$. Then,

$$\begin{aligned} \max_{x \in [\ell, u]} |p^*(x) - p(x)| &\leq \max_{x \in [\ell, u]} |1 - p(x)| + \max_{x \in [\ell, u]} |1 - p^*(x)| \\ &\leq 2 \max_{x \in [\ell, u]} |1 - p(x)| \\ &\leq 2(1 - \ell/u)^3. \end{aligned}$$

where we invoked [26, Theorem 3.1] and the fact that p^* is the optimal approximation to $x \mapsto 1$ from $\mathbb{P}_5^{\text{odd}}$. Hence, when $\ell/u \geq 1 - \epsilon_d^{1/3}$, where $\epsilon_{\text{double}} \approx 1.1 \times 10^{-16}$ is the double precision machine epsilon, then $|p^*(x) - p(x)| \leq 2\epsilon_{\text{double}}$. In other words, up to double precision machine epsilon, p^* is equal to p . Therefore, whenever $\ell/u \geq 1 - \epsilon_{\text{double}}^{1/3}$ the algorithm simply returns p as the optimal polynomial.

The algorithm is outlined in Algorithm 2. In our experiments, we never observed Algorithm 2 taking more than five iterations to converge.

Algorithm 2 Remez algorithm (degree 5 approximation for $\text{sign}(x)$)

input: interval $[\ell, u]$ for $\ell > 0$, initial trial points $x_1^{(1)}, x_2^{(1)} \in [\ell, u]$.

output: Approximation $p \in \mathbb{P}_5^{\text{odd}}$ to $p^* = \operatorname{argmin}_{p \in \mathbb{P}_5^{\text{odd}}} \max_{x \in [\ell, u]} |1 - p(x)|$.

define $\epsilon_{\text{double}} = 1.11 \times 10^{-16}$

if $\ell/u \geq 1 - \epsilon_{\text{double}}^{1/3}$ **then**

 Return $p(x) = \frac{x/u}{8} (15 - 10(x/u)^2 + 3(x/u)^4)$

end if

$E_0 = \infty, E_{-1} = -\infty$

$k \leftarrow 0$

while $||E_k| - |E_{k-1}|| > \epsilon_{\text{double}}$ **do**

$k \leftarrow k + 1$

$$\begin{bmatrix} a_k \\ b_k \\ c_k \\ E_k \end{bmatrix} = \begin{bmatrix} \ell & \ell^3 & \ell^5 & 1 \\ x_1^{(k)} & (x_1^{(k)})^3 & (x_1^{(k)})^5 & -1 \\ x_2^{(k)} & (x_2^{(k)})^3 & (x_2^{(k)})^5 & 1 \\ u & u^3 & u^5 & -1 \end{bmatrix}^{-1} \begin{bmatrix} 1 \\ 1 \\ 1 \\ 1 \end{bmatrix}$$

$$x_1^{(k+1)} = \sqrt{\frac{-3b_k - \sqrt{9b_k^2 - 20a_k c_k}}{10c_k}}, x_2^{(k+1)} = \sqrt{\frac{-3b_k + \sqrt{9b_k^2 - 20a_k c_k}}{10c_k}}$$

end while

Return $p(x) = a_k x + b_k x^3 + c_k x^5$

E Initialization for Matrices with Large Spectral Gaps

In Section 4, we constructed a sequence of polynomials that is adapted to the range of the singular values $[\ell, u]$. Assuming nothing else about the input, these polynomials are optimal because they provide a good approximation to 1 across the entire interval. However, in many applications, the spectrum has large gaps; that is, there are several large outlying singular values that are well-separated from the rest, . For these matrices, it is not necessary for the polynomial to be accurate on the entire interval $[\ell, u]$, only on the range of the small singular values plus a few large isolated points. In this section, we

take advantage of this structure to accelerate our method by preprocessing the matrix to eliminate the largest singular values.

The first step is to find small intervals containing each of these large singular values. To find lower bounds, we use subspace iteration, which is a generalization of the power method that approximates multiple singular values simultaneously. Fix k , the number of singular values we wish to eliminate. Letting $\sigma_1 \geq \dots \geq \sigma_n$ denote the singular values of \mathbf{M} , subspace iteration produces estimates $\tilde{\sigma}_1 \geq \dots \geq \tilde{\sigma}_k$ satisfying $\sigma_i \geq \tilde{\sigma}_i$ for all $i \in 1, \dots, k$.³ To find upper bounds on each σ_i , we can use the fact that $\|\mathbf{M}\|_F^2 = \sum_{j=1}^n \sigma_j^2$ as follows:

$$\sigma_i^2 = \|\mathbf{M}\|_F^2 - \sum_{j=1, j \neq i}^n \sigma_j^2 \leq \|\mathbf{M}\|_F^2 - \sum_{j=1, j \neq i}^k \sigma_j^2 \leq \|\mathbf{M}\|_F^2 - \sum_{j=1, j \neq i}^k \tilde{\sigma}_j^2 \quad (21)$$

That is, for each $i \in [n]$,

$$\sigma_i \in \left[\tilde{\sigma}_i, \sqrt{\|\mathbf{M}\|_F^2 - \sum_{j=1, j \neq i}^k \tilde{\sigma}_j^2} \right]$$

Setting $i = k + 1$, the above also provides an upper bound for the tail of the spectrum, $\sigma_{k+1}, \dots, \sigma_n$.

The second step is to find an odd polynomial that well-approximates the constant function on each of these intervals and on the tail simultaneously. For simplicity, we treat only the $k = 1$ case here. Assume that \mathbf{M} is normalized to $\|\mathbf{M}\|_F = 1$ and let $z = \tilde{\sigma}_1$ be the lower bound produced by subspace iteration (which reduces to the power method in this case). Then (21) gives $\sigma_1 \in [z, 1]$ and $\sigma_2, \dots, \sigma_n \leq \sqrt{1 - z^2}$. Assume that these intervals do not overlap, that is, $\sqrt{1 - z^2} \leq z \iff z \geq 1/\sqrt{2}$. Then we construct the unique odd cubic polynomial $p(x) = ax + bx^3$ that satisfies $p(\sqrt{1 - z^2}) = 1$ and $p(z) = 1$ by setting

$$a = \frac{z^2(z + \sqrt{1 - z^2}) - \sqrt{1 - z^2}}{z\sqrt{1 - z^2}(2z^2 - 1)} \quad b = \frac{\sqrt{1 - z^2} - z}{z\sqrt{1 - z^2}(2z^2 - 1)} \quad (22)$$

Because $p(0) = 0$ and p has at most one local extremum on $\mathbb{R}_{\geq 0}$, these conditions immediately guarantee that p is concave-increasing on $[0, \sqrt{1 - z^2}]$, so it must lie above the line $x \mapsto x/\sqrt{1 - z^2}$. Furthermore, p is decreasing on $[\sigma_1, 1]$, so it maps $\sigma_1 \in [z, 1]$ to $[p(1), 1]$. By minimizing $p(1)$ over all valid z s (that is, over the interval $[1/\sqrt{2}, 1]$), one can further show that $p(1) > 1/\sqrt{2}$, so σ_1 cannot be decreased very much by applying p . Thus, the largest singular value of $p(\mathbf{M})$ is still at most 1, while the smaller singular values have increased by a potentially large factor of $1/\sqrt{1 - z^2}$. When there is a large outlying singular value, z is close to 1 and this initialization scheme makes much more progress than a standard iteration of **PolarExpress** would have.

In Figure 7, we demonstrate the benefit of using the p given by (22) on a synthetic matrix whose spectrum follows a power law decay. That is, $\sigma_j(\mathbf{M}) = j^{-5}$. For both Newton-Schulz and **Polar Express** performing the extra spectrum-aware initialization step described in this section leads to significant speedups in convergence, even if we use one fewer iteration of the baseline method

³Let $\mathbf{Q}_0 \in \mathbb{R}^{n \times k}$ be a random matrix with orthonormal columns and define $\mathbf{Q}_{t+1}, \mathbf{R}_{t+1} = \mathbf{qr}(\mathbf{M}^\top \mathbf{M} \mathbf{Q}_t)$, where \mathbf{qr} is the QR decomposition. Subspace iteration outputs the singular values $\tilde{\sigma}_1, \dots, \tilde{\sigma}_k$ of $\mathbf{M} \mathbf{Q}_T$, $\tilde{\sigma}_1, \dots, \tilde{\sigma}_k$. By the Cauchy interlacing theorem, $\tilde{\sigma}_k \leq \sigma_k$.

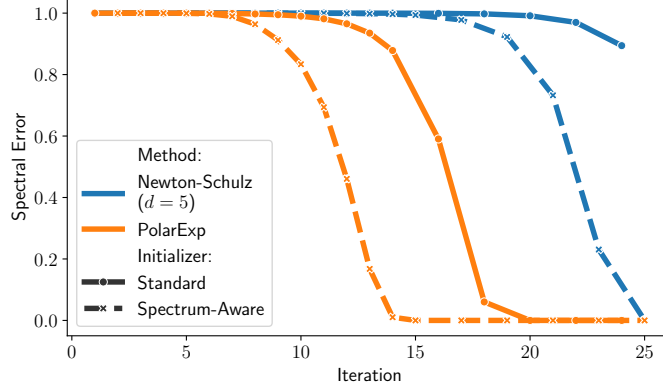


Figure 7: Benefits of the spectrum-aware initialization scheme of [Appendix E](#). Using this scheme improves convergence of both Newton-Schulz and Polar Express on a synthetic 32×32 matrix with $\sigma_j(\mathbf{M}) = j^{-5}$. Note that we count the spectrum-aware initialization as an additional iteration.

F Fast Polynomial Iteration for Rectangular Matrices

In this section, we describe a simple method for applying an iterative polynomial method to a rectangular matrix. For matrices with a large aspect ratio, this method yields significant computational savings. We emphasize that this method is applicable to *any* computation of the form $(p_T \circ \dots \circ p_1)(\mathbf{X})$, where each p_t is an odd polynomial.

As a preliminary, we first describe the baseline approach. Let $\mathbf{X} \in \mathbb{R}^{m \times n}$ with $m = \alpha n \geq n$, where $\alpha \geq 1$ is called the aspect ratio. Any odd polynomial p of degree $d = 2q + 1$ can be represented as $p(x) = xh(x^2)$, where h is a polynomial of degree q . Thus, $p(\mathbf{X}) = \mathbf{X}h(\mathbf{X}^\top \mathbf{X})$. Furthermore, h can be written in a factored form called Horner's rule to reduce the number of multiplications. For instance, if $h(y) = a + by + cy^2 + dy^3$, Horner's rule gives $h(y) = a + y(b + y(c + dy))$. For a matrix, $h(\mathbf{Y}) = a\mathbf{I} + \mathbf{Y}(b\mathbf{I} + \mathbf{Y}(c\mathbf{I} + d\mathbf{Y}))$. Thus for $\mathbf{Y} \in \mathbb{R}^{n \times n}$, computing $h(\mathbf{Y})$ costs about $(\deg(h) - 1) \cdot n^3$ operations, and computing $p(\mathbf{X}) = \mathbf{X}h(\mathbf{X}^\top \mathbf{X})$ costs $2mn^2 + \left(\frac{d-1}{2} - 1\right) \cdot n^3 = \left(\frac{d-3}{2} + 2\alpha\right) \cdot n^3$ operations. This process could be repeated for each iteration p_1, \dots, p_T . Notice that if we instead computed $h(\mathbf{X}\mathbf{X}^\top)\mathbf{X}$, the result would be the same but the cost would be higher.

A major drawback of this naive approach is that it has a strong dependence on α , since two rectangular matrix multiplications must be performed in *each* of the T iterations. When $m \gg n$, these two multiplications dominate the cost. In [Algorithm 3](#), we introduce a simple trick that dramatically reduces this cost, using just two rectangular matrix multiplications to compute *all* T iterations.

To see why this works, define $q_0(x) = x$,

$$q_t(x) = \frac{(p_t \circ \dots \circ p_1)(x)}{x} = \frac{p_t((p_{t-1} \circ \dots \circ p_1)(x))}{x} = \frac{p_t(xq_{t-1}(x))}{x} \quad (23)$$

$$= \frac{xq_{t-1}(x) \cdot h_t((xq_{t-1}(x))^2)}{x} = q_{t-1}(x) \cdot h_t(x^2 \cdot q_{t-1}(x)^2) \quad (24)$$

and $r_t(x) = x^2 \cdot q_{t-1}(x)^2$. It is clear by induction that $\mathbf{R}_t = r_t(\mathbf{X})$, $\mathbf{Q}_t = q_t(\mathbf{X})$, and $\mathbf{X}\mathbf{Q}_T = (p_T \circ \dots \circ p_1)(\mathbf{X})$. As promised, this algorithm uses no rectangular multiplications in the for-loop. If each p_t is degree d , then the total cost is $\left(\frac{d+3}{2}T + 2\alpha\right) \cdot n^3$. When

Algorithm 3 Fast Polynomial Iteration for Rectangular Matrices

input: $\mathbf{X} \in \mathbb{R}^{m \times n}$ with $m > 1.5n$, odd polynomials $p_1(x) = xh_1(x^2), \dots, p_T(x) = xh_T(x^2)$.

output: The matrix $(p_T \circ \dots \circ p_1)(\mathbf{X})$.

```
 $\mathbf{Y} = \mathbf{X}^\top \mathbf{X}$   $\triangleright mn^2$   
Let  $\mathbf{Q}_0 = \mathbf{I}$   
for  $t = 1, 2, \dots, T$  do  $\triangleright 2n^3$   
     $\mathbf{R}_t = \mathbf{Q}_{t-1}^\top \mathbf{Y} \mathbf{Q}_{t-1}$   $\triangleright \text{Horner's rule: } \deg(h_t) \cdot n^3$   
     $\mathbf{Q}_t = \mathbf{Q}_{t-1} h_t(\mathbf{R}_t)$   
end for  
return  $\mathbf{X} \mathbf{Q}_T$   $\triangleright mn^2$ 
```

$\alpha > 1.5 \frac{T}{T-1}$, this is smaller than the naive method. We can use this criterion to select either Algorithm 3 or the baseline method at runtime.

There is one significant weakness of Algorithm 3. In `bfloat16` precision, it can introduce numerical errors. Our intuition for why this happens is as follows. Let $\mathbf{X} = \mathbf{U} \mathbf{\Sigma} \mathbf{V}^\top$ be the SVD. For large T , $(p_T \circ \dots \circ p_1)(\mathbf{X}) = \mathbf{X} \mathbf{Q}_T \approx \text{polar}(\mathbf{X}) = \mathbf{U} \mathbf{V}^\top$. Thus, $\mathbf{Q}_T \approx \mathbf{V}^\top \mathbf{\Sigma}^{-1} \mathbf{V}$. When \mathbf{X} has very small singular values and the floating point precision is very low, instantiating \mathbf{Q}_T may be unstable. To mitigate this issue, we use a restarting strategy. Notice that the issue arises only for large T , for which $(p_T \circ \dots \circ p_1)(\epsilon) \approx 1$. Limiting ourselves to $T = 3$ iterations improves the conditioning of \mathbf{Q}_T because $(p_T \circ \dots \circ p_1)(\epsilon) \ll 1$. Thus, to compute $T = 6$ iterations, we can apply Algorithm 3 first to the first three polynomials, then again to the last three polynomials. Note that restarting Algorithm 3 after every iteration is exactly the same as the baseline method. This approach provides a tunable hyperparameter—the number of iterations we apply before restarting Algorithm 3—allowing us to find a balance between the fully stable but slow baseline on the one hand, and a very fast but numerically risky method on the other hand.

Figure 8 shows that using Algorithm 3 can dramatically improve runtime on the GPU when the aspect ratio is large enough. As expected, using Algorithm 3 for many iterations significantly reduces the dependence of the runtime on the aspect ratio. Running six iterations of a degree-5 polynomial method when $\alpha = 4$ (as with the linear transformations in each MLP block of a transformer) we obtain almost a 2x speedup, and when $\alpha = 32$, we obtain nearly a 10x speedup. If we restart every three iterations, the trend is the same but the runtimes savings are less.

Preliminary experiments using Algorithm 3 with `Muon` in `bfloat16` were not successful. The training and validation losses were sometimes significantly higher than before, even accounting for the runtime savings of Algorithm 3. While this technique may already be applicable in `float32` or for architectures whose weight matrices have larger aspect ratios, more work is needed to make it practical for general deep learning applications.

If these problems can be mitigated, the speed afforded by Algorithm 3 suggests a potentially beneficial change in the way `Muon` is applied to transformers. Each multi-head attention layer contains four square weight matrices $\mathbf{W}_Q, \mathbf{W}_K, \mathbf{W}_V$ and $\mathbf{W}_O \in \mathbb{R}^{d \times d}$. The orthogonalization step of `Muon` is either applied separately to these four matrices or else to $[\mathbf{W}_Q \mid \mathbf{W}_K \mid \mathbf{W}_V]$ and \mathbf{W}_O , since typical implementations of multi-head attention store the weights in this concatenated form. However, we believe it is natural to consider each of these four weight matrices to be a concatenation of many smaller linear transformations, each corresponding to a single attention head. If H is the number of heads, each of these

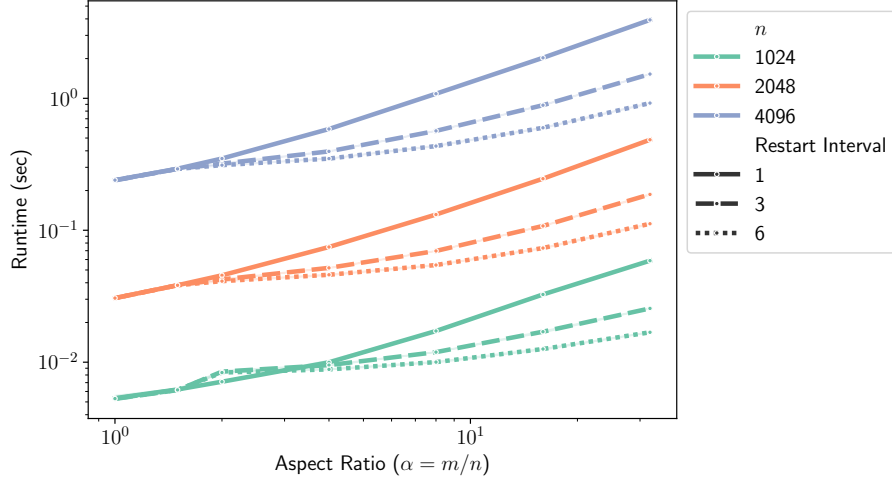


Figure 8: Effects of using [Algorithm 3](#) on runtime on a GPU. We run $T = 6$ iterations of a degree-5 polynomial method on matrices with various dimensions n and aspect ratios α . Restart interval 6 is [Algorithm 3](#), restart interval 1 is equivalent to not using [Algorithm 3](#), and restart interval 3 is an intermediate method that calls [Algorithm 3](#) once to do the first three iterations and again to do the last three iterations for greater stability. When $\alpha \gg 1$, increasing the restart interval makes the runtime many times faster.

smaller matrices has size $d \times \frac{d}{H}$; that is, they have aspect ratio $\alpha = H$. Since typical transformers like GPT-3 can have as many as 96 heads, this version of **Muon** can yield huge savings in the runtime of each step. We leave it to future work to examine whether this version of **Muon** also enjoys fast convergence.

G Code for Constructing Polynomials of Polar Express

The following code gives a Python implementation of the offline stage of [Algorithm 1](#). This code was used to construct the coefficients of the polynomials given in (17), which in turn were used in our **Muon** experiments ([Section 5.2](#)). It uses $\ell = 10^{-3}$ and $u = 1$ by default. It incorporates [Algorithm 2](#) and the numerical tweaks described in [Section 4.4](#)

```
from math import inf, sqrt
import numpy as np

def optimal_quintic(l, u):
    assert 0 <= l <= u
    if 1 - 5e-6 <= 1 / u:
        # Above this threshold, the equioscillating polynomials
        # is numerically equal to...
        return (15/8)/u, (-10/8)/(u**3), (3/8)/(u**5)
    # This initialization becomes exact as l -> u
    q = (3*l + 1) / 4
    r = (1 + 3) / 4
    E, old_E = inf, None
    while not old_E or abs(old_E - E) > 1e-15:
        old_E = E
        LHS = np.array([
```

```

        [1, l**3, l**5, 1],
        [q, q**3, q**5, -1],
        [r, r**3, r**5, 1],
        [u, u**3, u**5, -1],
    ])
    a, b, c, E = np.linalg.solve(LHS, np.ones(4))
    q, r = np.sqrt((-3*b + np.array([-1, 1]) *
        sqrt(9*b**2 - 20*a*c)) / (10*c))
    return float(a), float(b), float(c)

def optimal_composition(l, num_iters, cushion=0.02407327424182761):
    u = 1
    coefficients = []
    for _ in range(num_iters):
        a, b, c = optimal_quintic(max(l, cushion*u), u)
        # Due to cushioning, this may be centered around 1 with
        # respect to 0.024*u, u. Recenter it around 1 with respect
        # to l, u, meaning find c so that 1 - c*p(l) = c*p(u) - 1:
        pl = a*l + b*l**3 + c*l**5
        pu = a*u + b*u**3 + c*u**5
        rescalar = 2/(pl + pu)
        a *= rescalar; b *= rescalar; c *= rescalar
        # Safety factor:
        a /= 1.01; b /= 1.01**3; c /= 1.01**5
        coefficients.append((a, b, c))
        l = a*l + b*l**3 + c*l**5
        u = 2 - l
    return coefficients

print(*optimal_composition(1e-3, 10), sep="\n")

```